Contents

European Centre for Medium-Range Weather Forecasts
Shinfield Park, Reading, Berkshire RG2 9AX, UK
Fax: . . . . . +44 118 986 9450
Telephone: National 0118 949 9000
International . . . . . +44 118 949 9000
ECMWF Web site . . . . . .http://www.ecmwf.int

The ECMWF Newsletter is published quarterly. Its purpose is to make users of ECMWF products, collaborators with ECMWF and the wider meteorological community aware of new developments at ECMWF and the use that can be made of ECMWF products. Most articles are prepared by staff at ECMWF, but articles are also welcome from people working elsewhere, especially those from Member States and Co-operating States. The ECMWF Newsletter is not peer-reviewed.

Editor: Bob Riddaway

Typesetting and Graphics: Rob Hine

Front cover

Images associated with the measurements of GPS radio occultation using the array of COSMIC satellites.

Images *Courtesy of the Orbital Science Corporation*.

EDITORIAL

Access to the TIGGE database

THORPEX is a WMO initiative to accelerate improvements in the accuracy of one-day to two-week high-impact weather forecasts for the benefit of society, economy and the environment. A strong participation to THORPEX is an important element of the ECMWF Strategy 2006-2015.

There are many ECMWF contributions to THORPEX, but developing the infrastructure for TIGGE, the THORPEX Interactive Grand Global Ensemble, is probably the most important. Following a recommendation of the THORPEX International Research Implementation Plan, ECMWF hosted an international workshop in March 2005 to agree the concept and the roadmap for TIGGE. The main objective of TIGGE is to create a database of operational ensemble forecasts from all major forecasting centres, and to give access to this database to a wide international community for investigating the skill of multi-model ensembles, especially for high-impact weather, and developing new applications of ensemble forecasts. This should ultimately evolve into a real-time Global Interactive Forecasting System (GIFS), which is considered one of the major deliverables of THORPEX. TIGGE is also one deliverable of the GEO work plan.

The first phase of TIGGE calls for the accumulation of global ensemble forecasts produced by all operational centres in identical databases located at ECMWF, NCAR (USA) and CMA (China). These databases will be made accessible to scientists in near-real time. ECMWF has led the development of the infrastructure for this first phase, in collaboration with the other archive centres. In 2006, the content and the format of the archive, as well as the data transmission protocols, were agreed with the eleven global NWP centres that will provide data to TIGGE. The total volume to be transferred is about 300 GBytes/day, and comprises global fields of about 70 parameters every 6 hours at native forecast resolution for each ensemble member. This is a significant technical challenge, and the difficulty of keeping this database consistent and complete must not be underestimated.

The IT experts of the three archive centres have been working hard since mid 2005 to develop the project, and the data providers have also worked hard to prepare their data in TIGGE-compliant format and to implement the transmission protocols. The first data reached the databases in autumn 2006, and the number of fields and data providers is increasing steadily. It is expected that the database will be nominal before the end of 2007.

Data distribution started at NCAR recently and is about to start at ECMWF. Watch http://tigge.ecmwf.int! The data will be accessible at no charge and usable for education and research as early as 48 hours after each forecast is issued. The Internet server will allow users to sign in, accept the data usage conditions, and download data. The initial functionalities for data access will be limited, but the quality of the service will increase with time, and quickly allow user-friendly access to significant data volumes.

At this exciting time of initial TIGGE service, it is a pleasure for me (also in my capacity as co-chair of the THORPEX GIFS-TIGGE Working Group) to congratulate and thank colleagues from all partner organizations for their hard work since 2005. I look forward to a rapid development of the use of TIGGE data and to the demonstration of new advances in forecast skill and applications of ensemble forecasts made possible by this project.

Philippe Bougeault

New items on the ECMWF web site

ANDY BRADY

Third Eumetcal Workshop

The Third Eumetcal Workshop and Advisory Board meeting will be held from 29 to 31 August 2007 at ECMWF. The aim of the Eumetcal workshop is to bring trainers, training managers and other meteorological staff dealing with training issues under the same roof to discuss and share ideas about current and evolving training techniques and to give the Eumetcal programme management important feedback on desired training resources.

www.ecmwf.int/newsevents/meetings/workshops/2007/EUMETCAL/

Hardware upgrades improve response of ECMWF web site

The web server hardware of the ECMWF web site was over five years old at the end of 2006. During the past five years the content and use of the web site has grown considerably. To maintain the service, a significant upgrade of our web server hardware to the latest IBM "Series x" servers (running Linux) was successfully completed during January. This has resulted in a significant improvement in the response of our web site, particularly for the popular charts and "your room" areas.

www.ecmwf.int/publications/cms/get/ecmwfnews/chewbacca

ECMWF Grib API 1.0 released

The new GRIB API software for encoding and decoding of WMO FM-92 GRIB edition 1 and edition 2 messages has been released. It consists of a program interface (grib_api) accessible from C and Fortran programs and a useful set of command line tools to quickly manipulate data in grib format.

www.ecmwf.int/products/data/software/grib_api.html

Ocean analysis

The web pages of the ocean analysis now include daily products from the latest ocean analysis as well as products from the historical reanalysis, going back to 1959. The pages also provide charts of observation coverage and quality control decisions.

www.ecmwf.int/products/forecasts/d/charts

ECMWF Seasonal Forecast System 3

The seasonal forecast pages have been significantly modified and reorganised with the implementation of System 3 of the ECMWF Seasonal Forecast. In addition annual range products are now available.

www.ecmwf.int/products/forecasts/d/charts/seasonal/forecast/

New layout of ECMWF front page

The front page of the ECMWF web site has been revised and now includes more timely detail on "ECMWF news" as well as references to articles in the *ECMWF Newsletter*. The information "About ECMWF" is now only available under the "About" section of our web site.

www.ecmwf.int/

Use and Interpretation of ECMWF Products

The objective of the course on "*Use and interpretation of ECMWF products*" is to assist Member States and Co-operating States in advanced training on the operational aspects of the ECMWF forecasting system. The course will be given twice in 2007, plus an additional module specifically for WMO Member States. The date for the second session (MET OP-II) is 4–8 June 2007. The course for WMO Members (MET OP-WMO) will be held on 15–19 October.

www.ecmwf.int/newsevents/training/2007/Products/

IIth Workshop on Meteorological Operational Systems

The 11th Workshop on Meteorological Operational Systems will be held from 12 to 16 November 2007. The objective of the workshop is to review the state of the art of meteorological operational systems and to address future trends in the use and interpretation of medium and extended range forecast guidance, operational data management systems and meteorological visualisation applications.

www.ecmwf.int/newsevents/meetings/workshops/2007/MOS_11/

Invitation to Tender ECMWF/2007/I92 published

At its session in December 2006, the ECMWF Council approved the acquisition process and budgetary framework (which included a considerable increase over ECMWF's current budget) for the procurement of a replacement High Performance Computing Facility (HPCF). An Invitation to Tender has been issued with a closing date of 1 June 2007.

www.ecmwf.int/newsevents/itt/2007-192/

Changes to the operational forecasting system

DAVID RICHARDSON

Testing of Cy32r2

A new cycle of the ECMWF forecast and analysis system has undergone extensive testing. This version includes the following changes.

- Three-minimization version of 4D-Var assimilation scheme (T95/T159/T255) with improved moist linear physics (cloud and convection).
- Improved parametrization of the heterogeneous ozone chemistry.
- New short-wave radiation scheme (RRTM-SW), plus McICA cloud-radiation interaction and MODIS albedo.
- Retuned ice particle size.
- Revised subgrid-orography scheme.
- Explicit numerical treatment of convection in the moist tangent linear model used in the calculation of tropical singular vectors.

This version has now been upgraded to include additional technical changes, including code optimisation, and the resulting Cycle 32r2 is now being tested.

New seasonal forecasting system, System 3

A new seasonal forecasting system, System 3, was introduced in March 2007. A scientific and technical description of System 3, including an assessment of performance, was presented in the Winter 2006/07 edition of the *ECMWF Newsletter*. An article item on page 28 of this edition of the newsletter describes some of the products available in the new system.

Moroccan Secretary of State visits ECMWF

MANFRED KLÖPPEL

ABDELKBIR ZAHOUD, Secretary of State to the Ministry of Territorial Development, Water and Environment in Charge of Water of the Kingdom of Morocco, paid a visit to the ECMWF on 7 March 2007. He was accompanied by Mustapha Geanah, Director of the Moroccan National Weather Service, and Dalil Guendouz, Director of l'Ecole Hassania des Travaux Publics.

Dominique Marbouty, Director of ECMWF, welcomed the visitors and, together with several staff members, gave an overview of the Centre's facilities and main research and operational activities. Emphasis was put on the accuracy of the Centre's forecasting system, the intense use of satellite data, and its supercomputing expertise.

Morocco became the first non-European Co-operating State on 1 December 2006 see:

http://www.ecmwf.int/publications/cms/get/ecmwfnews/170

Mr. Zahoud said: "I am impressed by the scientific expertise and the high standard of the technical infrastructure established at the European Centre for Medium-Range Weather Forecasts. I am convinced that the use of the Centre's medium-range and seasonal weather forecasts will benefit the people of Morocco. I am confident that the Moroccan National Weather Service will profit from close collaboration with the Centre."

Dalil Guendouz, Dominique Marbouty, Abdelkbir Zahoud and Mustapha Geanah

METEOSAT-9: The new prime satellite at 0° longitude

JEAN-NOËL THÉPAUT

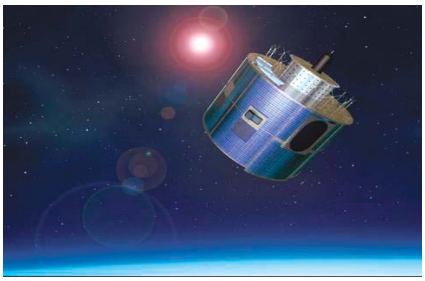

METEOSAT-9 is the second of the four geostationary satellites forming the EUMETSAT Meteosat Second Generation (MSG) programme. This programme will operate until 2018, serving the needs of ECMWF (among many other users) by providing meteorological products, in particular Atmospheric Motion Vectors (AMVs) and Clear-Sky Radiances (CSRs).

Meteosat-9 was successfully launched in December 2005 and started imaging soon after. ECMWF started to receive Meteosat-9 products in June 2006. Since then AMVs and CSRs from this satellite have been monitored routinely as it is the official back-up satellite to Meteosat-8. The monitoring statistics of AMV and CSR products have revealed a very similar quality between Meteosat-8 and Meteosat-9, to such an extent that Meteosat-9 was used operationally at ECMWF between 28 September and 18 October 2006, following the unavailability of Meteosat-8 products during some of this period.

Following an announcement by EUMETSAT that Meteosat-9 would become the prime satellite at 0° longitude as of 11 April 2007, and due to the good performance of the SEVIRI instrument onboard, it was decided to move the active assimilation of AMV and CSR products at ECMWF from Meteosat-8 to Meteosat-9. This change occurred on 27 March.

Monitoring of SSMIS from DMSP-16 at ECMWF

NIELS BORMANN, GRAEME KELLY

THE FIRST Special Sensor Microwave Imager/Sounder (SSMIS) instrument was launched onboard the polar-orbiting Defense Meteorological Satellite Program (DMSP) platform F-16 on 18 October 2003. SSMIS is the operational follow-on instrument to SSMI with significantly extended capabilities. This novel instrument provides information on temperature and humidity profiles, rain, and surface properties, by sensing microwave radiation emitted from the Earth's surface and atmosphere. The SSMIS combines three instruments in one, by observing at sounding frequencies previously available from AMSU-A and AMSU-B/MHS, and at imaging frequencies that were previously available from SSMI. SSMIS also provides previously unavailable channels sensitive to mesospheric temperature. In contrast to the cross-track scanning AMSU-A and AMSU-B/MHS instruments, the SSMIS views the Earth under a constant angle, similar to the SSMI instrument. This so-called conical-scan geometry allows observations to be taken at fixed polarisation states, providing additional information on the Earth's surface.

During the calibration/validation phase for SSMIS, it was found that the F-16 instrument has two serious anomalies.

- At times, solar light intrudes onto the instrument's calibration load, therefore leading to erroneous results for the calibration. Reliable calibration is crucial for the quantitative use of the data.
- The large reflector necessary for the conical-scanning geometry emits more radiation than previously expected, and this radiation was difficult to model during the day/night transitions during one orbit.

NWP played a paramount role in characterising and flagging or correcting the SSMIS observations. Routine comparisons between SSMIS radiances and model equivalents clearly showed the bias signatures arising from the solar intrusion and the reflector emission problems. Using these bias signatures and computer-modelling of the SSMIS instrument, Bill Bell (UK Met Office) and others identified the areas for which data are affected by solar intrusions and where the data therefore should not be used. In the case of the reflector emission signatures, comparisons to NWP data were used to estimate the emissivity of the SSMIS reflector, and to develop a simple correction model for the reflector emissions. Both aspects are implemented in the pre-processor for SSMIS radiances developed at the Met Office.

As soon as data were made available in mid-2005, ECMWF began monitoring and assimilation experiments using the Met Office pre-processed radiances to provide independent feedback on the performance of the flagging and the correction schemes. The data has been operationally monitored at ECMWF since 12 December 2006. Monitoring results indicate that the pre-processed data has very good noise characteristics for the temperature sounding channels. However, some local biases related to the instrument anomalies are still present and can be as large as the noise. ECMWF is in continuous dialogue with the Met Office to further improve the corrections and the usability of the data. For the SSMI-like imaging channels, the instrument problems are less severe, and operational assimilation of these channels will start in summer 2007. Assimilation of these channels will further improve the ECMWF analyses of total water vapour, and ensure the continuation in the use of these important measurements beyond SSMI.

The F-16 SSMIS is the first in a series of five instruments to be flown on DMSP satellites. The second instrument was successfully launched onboard F-17 on 4 November 2006. The experience with the F-16 SSMIS data at NWP centres and elsewhere has led to improvements in the instrument design for the F-17 SSMIS. ECMWF will commence operational monitoring of F-17 SSMIS data as soon as they are made available to us.

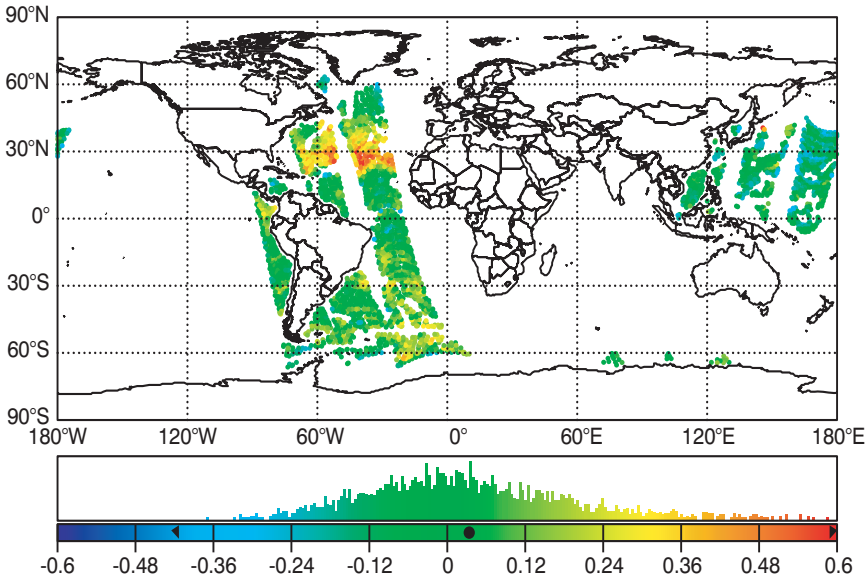

Observed minus simulated brightness temperatures [K] for SSMIS channel 3 (53.596 GHz V) for a six-hour period at around 00 UTC on 3 April 2006. Gaps in the orbits are due to solar intrusion flagging. Areas of local positive biases are apparent over the Northern Atlantic. These coincide with the satellite's emergence from the Earth's shadow, leading to rapid changes in the reflector emissions. Such areas are now flagged in the Met Office pre-processor, after feedback from ECMWF and other NWP centres.

Update on ERA-Interim

ADRIAN SIMMONS, SAKARI UPPALA, DICK DEE

AN INTRODUCTION to ERA-Interim was given in the last issue of the *ECMWF Newsletter No. 110* (Winter 2006/07). The primary reanalysis stream has progressed well since then, with 1994 completed by early April and production running at a rate close to one year of reanalysis per calendar month.

MARS users may access a provisional set of products for the years 1989–1992 by specifying *EXPVER = 5* and *class = EI* in their retrieval request. Other users may obtain these products from ECMWF's Data Services. These data have been made available for early exploratory use only, and the provisional nature of the data should be identified in reporting any results obtained from them. The analyses for these four years are currently being rerun to correct a number of small problems that were detected and remedied on-the-fly in the original production stream. The rerun also includes a change to the assimilation of the highest-sounding radiances from the Stratospheric Sounding Unit (SSU) on the NOAA polar-orbiting satellites, a change that was made in the primary production stream when it reached the end of 1992.

The latter change comprises removal of bias correction from SSU channel-3 radiances. Upper-stratospheric temperatures are thereby reduced by several degrees Kelvin, but remain higher than in ERA-40, and are now more consistent with other climatologies. The principal change below 10 hPa occurs in the Antarctic winter vortex, where temperature varies more smoothly with height. The accompanying pressure/latitude cross-sections of zonal-mean temperature illustrate these features for July 1993, for an analysis using the original production system (left) and for the analysis from the revised production system (right).

A small drying of the atmosphere and reduction in rainfall in the background forecasts (bringing global-mean precipitation and evaporation close to balance) occurs at the end of 1991. This is most likely associated with a change in the source of rain-affected SSMI radiance data from the DMSP-8 satellite to DMSP-10, but this remains to be confirmed.

A second release of products from ERA-Interim will be made once the years 1989 to 1992 have been repeated. It will encompass not only the revised analyses for these four years but also the corresponding analyses for several years following 1992.

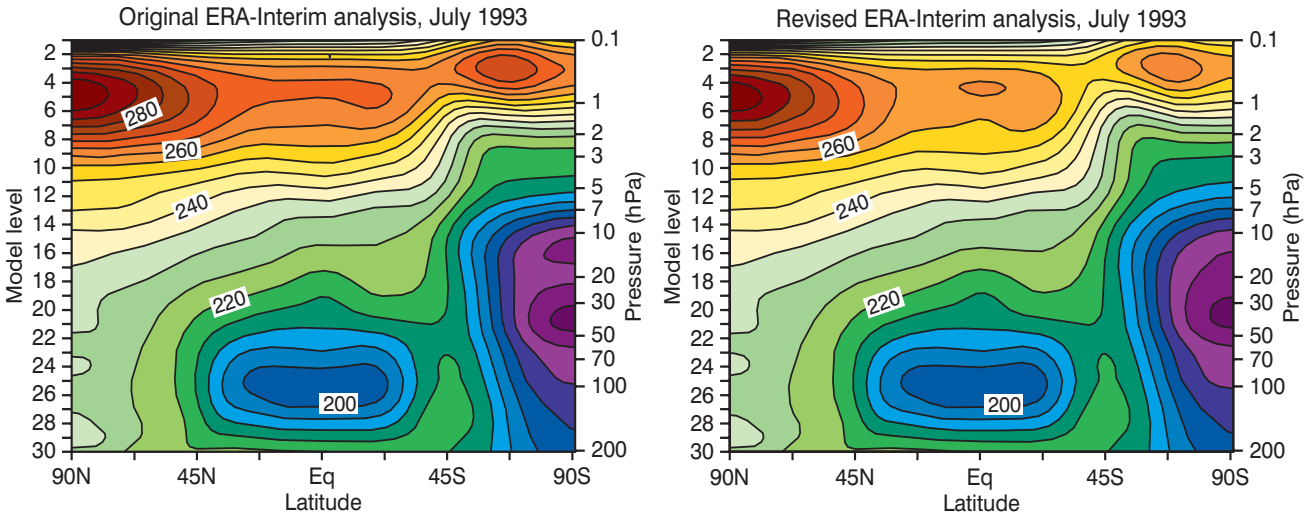

Pressure/latitude cross-sections of zonal-mean temperature for July 1993 for an analysis using the original production system (left) and for the corresponding analysis from the revised production system which has the bias correction from SSU channel-3 radiances removed (right).

Operational assimilation of GPS radio occultation measurements at ECMWF

SEAN HEALY

ECMWF became the first operational centre to assimilate GPS radio occultation (GPSRO) measurements from COSMIC satellites on 12 December, 2006. These measurements produce significant improvements in stratospheric temperature and height biases, particularly in the southern hemisphere.

The GPSRO measurements are globally distributed, have good vertical resolution and an all-weather capability. They are assimilated without bias correction and therefore provide potentially important "anchor points" for the recently introduced variational bias correction scheme (see *McNally et al.*, 2006, *ECMWF Newsletter No. 107*). The information content of the GPSRO measurements is complementary to that of high-resolution sounders, such as AIRS and IASI.

The first operational results at ECMWF, assimilating GPSRO measurements, have been very encouraging. They indicate that these measurements are a useful addition to the global observing network.

Background

The radio occultation measurement technique was pioneered by the planetary science community in the 1960s, and formed part of NASA's Mariner 3 and 4 missions to Mars. The measurement is based on observing how the paths of radio waves propagating through an atmosphere are bent as a result of refractive index gradients. The original concept envisaged by the planetary scientists was a fleeting, fly-by encounter, as a spacecraft passed behind a planet, but it was noted as early as 1965 that the method could be adapted to study the Earth's atmosphere. However, the required infrastructure – a constellation of radio transmitters orbiting the Earth – was considered unaffordable at that time.

In the late 1980s it was recognised that the 24 GPS satellites – primarily designed as a tool for precise positioning and navigation – would be a suitable source of radio signals, and the concept of GPS radio occultation (GPSRO) began to be explored. In 1995, work at the University Corporation for Atmospheric Research (UCAR) and the Jet Propulsion Laboratory (JPL) culminated in the launch of the "proof of concept" GPS/MET instrument into a low earth oribit (LEO). This mission placed a GPS receiver developed at JPL in space, and enabled the first GPSRO measurements to be made.

Figure 1 shows the geometry of the GPSRO measurement technique. A radio signal is transmitted by a GPS satellite, passes through the atmosphere and is measured with a GPS receiver placed on a LEO satellite, such as GPS/MET. The path is bent as a result of gradients in the refractive index of the atmosphere, which in turn can be related to gradients in the temperature and humidity. The ray bending angle, α, can be derived from the time required for the radio signal to propagate between the GPS and LEO satellites, and the motion of the LEO satellite enables the variation of α as a function of tangent height to be determined. Temperature and humidity information can be derived from the bending angle profiles. The limb sounding geometry of the measurements means that they have good vertical resolution, focussed around the tangent point. They are also less prone to biases than other satellite measurements because they are based on the precise measurement of a time delay. Furthermore, the forward modelling is relatively simple and it is not reliant on spectroscopic parameters, or the assumed concentrations of well mixed gases, which can produce biases in simulated satellite radiances.

The GPS/MET experiment was considered to be a major success. It demonstrated temperature profiles derived from GPSRO measurements were of sub-Kelvin

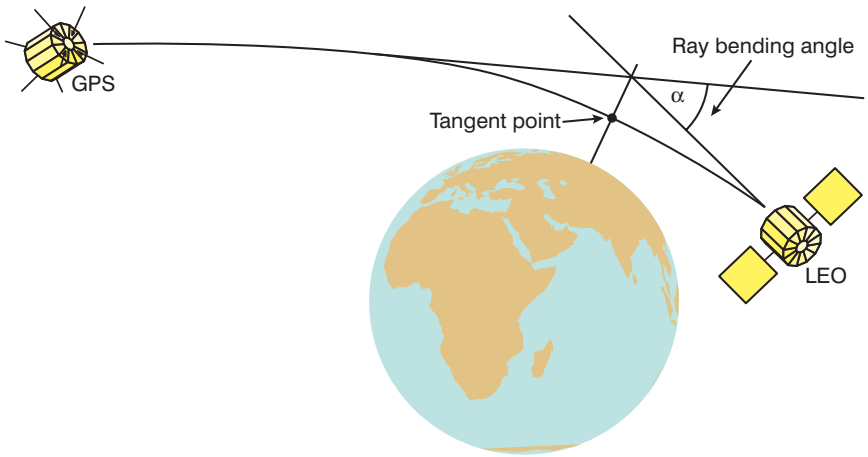

Figure 1 Geometry of a GPS RO measurement. A radio signal is emitted by the GPS satellite and measured with a receiver placed on the LEO. The path of the radio signal is bent as a result of refractive-index gradients in the atmosphere. The motion of the LEO satellite enables the variation of ray-bending with tangent height to be investigated.

accuracy for heights between 7 and 25 km, and this had important consequences.

- It led to a number of missions of opportunity, most notably CHAMP, which has provided GPSRO measurements since 2001.
- The GRAS GPSRO instrument was included on METOP, and it will provide operational data in 2007.
- The COSMIC proposal was formulated. This suggested placing the latest GPS receivers on a constellation of six LEO satellites, to provide ~2,500 globally distributed measurements per day, with near real time availability.

The COSMIC mission (full title Formosat-3/COSMIC) is a joint US/Taiwanese venture. The six COSMIC LEO satellites were launched on 14 April, 2006 from Vandenberge Air Force Base in California. Although it will take until late 2007 for the constellation to reach its final orbital configuration, which is designed to optimise the sampling across the globe (see Figure 2), the measurements have been made available to the general community since 28 July, 2006.

Assimilation of GPSRO measurements at ECMWF

The assimilation of GPSRO measurements in numerical weather prediction (NWP) systems was first investigated at ECMWF by John Eyre in 1994. This work is considered to be important within the GPSRO community because it placed the occultation measurements within the context of variational assimilation for the first time. Also it introduced the community to the philosophy that the assimilated quantity should be as close to the actual observation as possible. The work concluded that the GPSRO measurements were potentially useful for NWP and that the direct assimilation of bending angle profiles was probably the best strategy for using the data. However, further progress at that time was difficult because there was no foreseeable date when the GPSRO measurements would be become routinely available for assimilation at operational centres. The subsequent success of the GPS/MET and CHAMP missions, and then the possibility of receiving measurements from COSMIC and GRAS in near-real-time, changed this situation. Therefore, recently ECMWF's Integrated Forecast System (IFS) has been modified to enable the assimilation of limb sounding measurements (see *Bormann & Healy*, 2005, *ECMWF Newsletter No. 105*), including GPSRO bending angles.

Two bending angle observation operators are implemented in the IFS.

- ***One-dimensional operator***. The simplest operator provides a one-dimensional (1D) estimate of the bending angles. Essentially, this means that the two-dimensional, limb geometry of the measurement is ignored, and the bending is calculated using NWP profile information extracted at a single horizontal location, at the assumed tangent point location. The 1D bending angle operator used at ECMWF was developed by the EUMETSAT GRAS Satellite Application Facility (SAF) and will be available from the Met Office as part the Radio Occultation Processing Package (ROPP).
- ***Two-dimensional operator***. The second bending observation operator is two-dimensional (2D), meaning that it uses NWP profile information extracted at a series of horizontal locations within a 2D planar slice of the atmosphere. This should reduce forward model error as a result of a more physically realistic simulation of the problem.

The 2D operator has been used in a series of forecast impact experiments with CHAMP measurements, but it requires further testing with COSMIC data before it is considered for use in operations at ECMWF. However, note that it will form part of ECMWF's contribution to future upgrades of the GRAS-SAF's ROPP from 2008.

GPSRO Assimilation Experiments

The pre-operational GPSRO experiments assimilate measurements from COSMIC, CHAMP and GRACE-A with the 1D bending angle observation operator. One of the novel aspects of the COSMIC mission is the ability to measure both rising and the more conventional setting occultations. In a rising occultation the LEO satellite emerges from behind the Earth, and progressively higher regions of the atmosphere are probed. The error characteristics of rising occultations are still under investigation and therefore they are not assimilated in

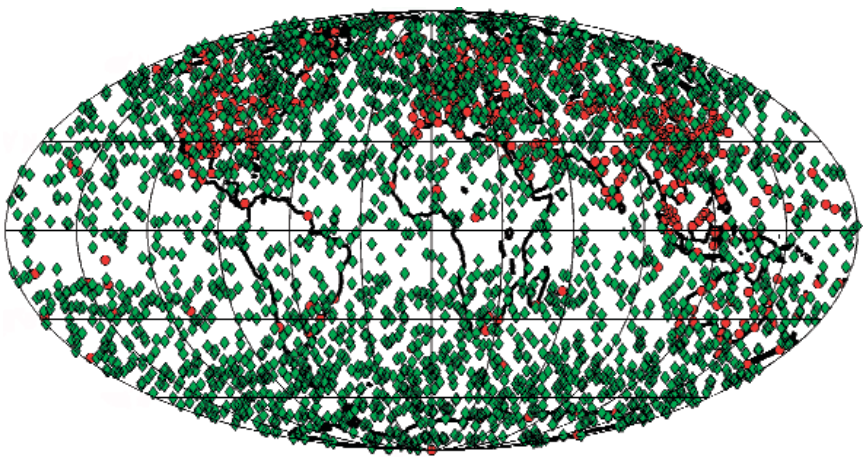

Figure 2 Global distribution of 2,500 COSMIC GPSRO measurements (green diamonds) over a 24-hour period, when the six satellites have reached their final orbital configuration. The red dots show the radiosonde network.

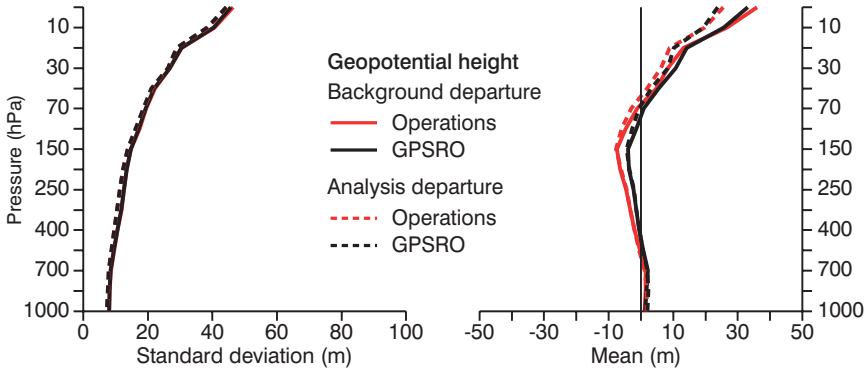

Figure 3 Standard deviation and mean of the forecast and analysis departures for radiosonde geopotential height measurements in the southern hemisphere for the GPSRO experiment and operations. The statistics are based on data from 81 radiosonde sites.

the pre-operational experiments. The COSMIC measurements assimilated at ECMWF are processed at UCAR and are routed to ECMWF via NESDIS and the Met Office. The CHAMP and GRACE-A measurements are now made available in near-real-time by GFZ Potsdam, as a result of a project funded by the German Ministry of Education and Research.

Studies about theoretical information content, and early research experiments with measurements from CHAMP, have shown that GPSRO measurements should have a significant impact on upper-tropospheric and lower/mid-stratospheric temperatures, particularly in the southern hemisphere. In these assimilation experiments, the GPSRO measurements have a neutral impact in the lower troposphere, but they produce a clear positive impact in the stratosphere. The GPSRO measurements improve known stratospheric height and temperature biases.

Figure 3 shows the standard deviation and mean of the background departure (observation minus background) and analysis departure (observation minus analysis) for radiosonde height measurements in the southern hemisphere. Although the standard deviations are similar for operations and the GPSRO experiment, there is a clear improvement in the mean departures between 400 hPa and 70 hPa. It is important to note that the GPSRO measurements are assimilated without any bias correction, and therefore it is encouraging to see

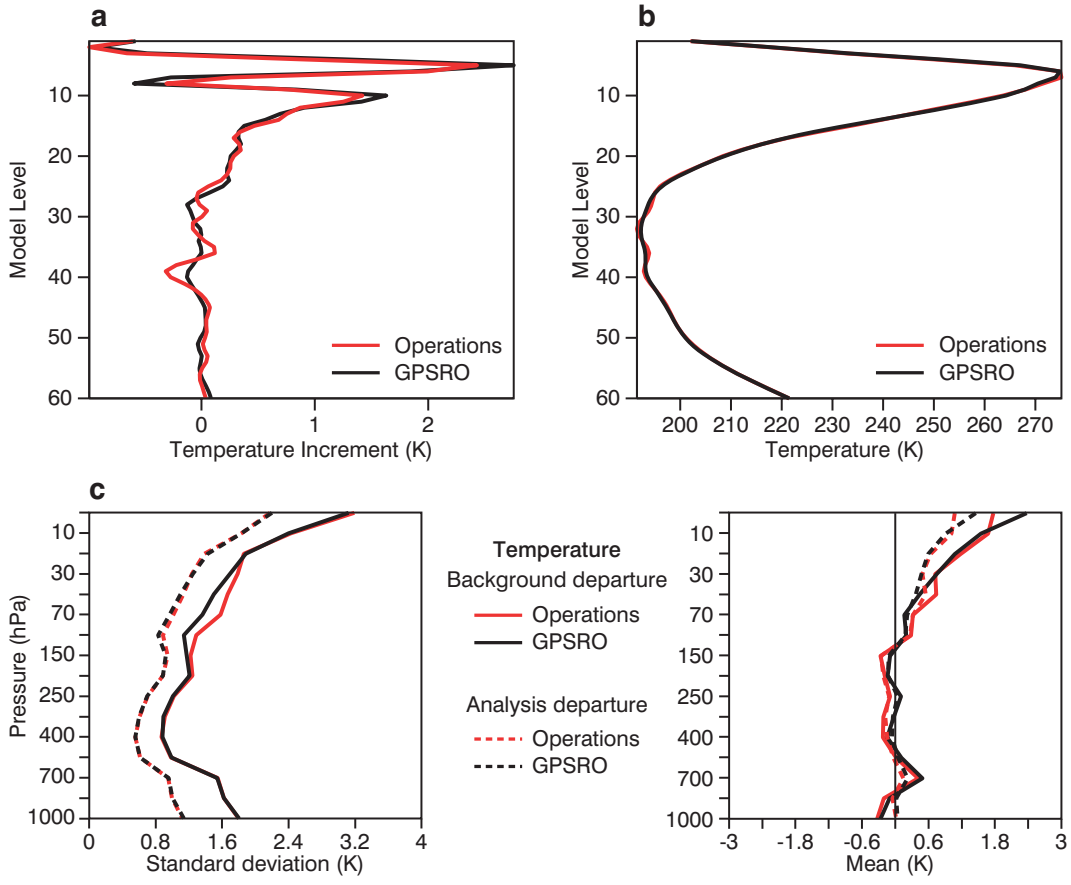

Figure 4 A vertical profiles of (a) mean temperature increments and (b) mean temperature analysis over the Antarctica on the uppermost 60 model levels for the GPSRO experiment and operations. (c) Shows the fit to radiosonde temperature measurements from 12 sites in Antarctica.

that assimilating these data improves the fit to radiosonde measurements. This also supports the idea that GPSRO should provide "anchor points" for the variational bias correction scheme by preventing the bias correction scheme from drifting to the climate of the NWP model.

Figures 4(a) and 4(b) show the mean temperature increments and mean analysis state, respectively, for the GPSRO experiment and operations over Antarctica averaged over period 14 to 30 September, 2006. The operational temperature analysis over Antarctica has been prone to spurious oscillations in the stratosphere. These oscillations arise as a result of large, systematic temperature increments in the upper stratosphere caused by NWP model error, which are propagated downwards in the analysis, as a result of the correlations in background error covariance matrix. The oscillations are problematic because they are in the "null-space" of satellite radiance measurements. This essentially means that the radiances have no sensitivity – or are "blind" – to these perturbations, because they are averaged out by the broad vertical weighting functions. In contrast, the GPSRO measurements have very good vertical resolution and they can both resolve and then correct these unphysical oscillations in the analysis. The large increments near the model top are not affected significantly by the introduction of the GPSRO measurements, but they do constrain the increments that cause the oscillations lower down. Furthermore, Figure 4(c) shows that assimilating the GPSRO measurements generally improves the fit to radiosonde temperature measurements over Antarctica.

Improvements in the stratospheric temperature analyses improve the subsequent temperature forecasts. Figure 5 shows the forecast fit to radiosonde temperature measurements in the southern hemisphere at 200, 100 and 50 hPa. The improvements at 100 hPa and 50 hPa are statistically significant at the 5% level over the day-1 to day-5 forecast range. There are also statistically significant improvements at 100 hPa in the northern hemisphere and tropics.

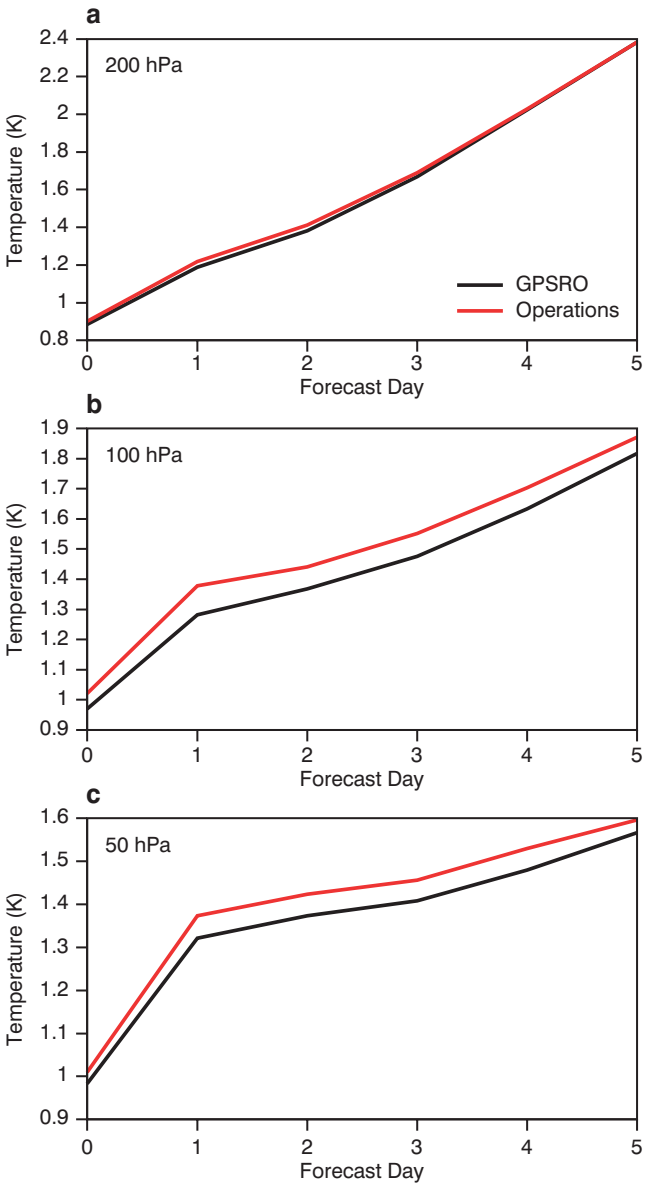

Figure 5 The r.m.s. fit to radiosonde temperature measurements over the southern hemisphere at (a) 200, (b) 100 and (c) 50 hPa over the day-1 to day-5 forecast range, for the GPSRO experiment and operations. The statistics are based on data from 61 radiosonde sites.

Implementation in operations

The COSMIC, CHAMP and GRACE-A GPSRO measurements became operational on 12 December, 2006, with the introduction of IFS cycle 31r2 (referred to as Cy31r2). The measurements have clearly improved some of the stratospheric height and temperature biases in the operational analyses. For example, Figure 6 shows a time series of the mean and standard deviation of the background and analysis departures from operations for radiosonde height and temperature measurements at 100 hPa in the southern hemisphere. The period starts on the first full day of Cy31r1 in operations, contains the change to Cy31r2 on 12 December and continues to the end of February, 2007. There is a clear improvement in the mean background departure for the radiosonde measurements with the introduction of Cy31r2. Similar improvements in the fit to radiosonde temperatures at 100 hPa are also evident in the northern hemisphere and tropics, although the magnitude is somewhat smaller. The vertical temperature oscillations over Antarctica have also been suppressed in Cy31r2.

Future work

The COSMIC, CHAMP and GRACE-A GPSRO measurements have been successfully assimilated in operations and measurements from GRAS will be available soon. ECMWF will monitor bending angle measurements from GRAS as soon as they become available, with a view to assimilating the data at the earliest opportunity. In addition, the exploitation of the existing data will be improved. For example, we currently assimilate over 1,000 occultations per day, but COSMIC is often producing over 800 rising occultations, which are not used.

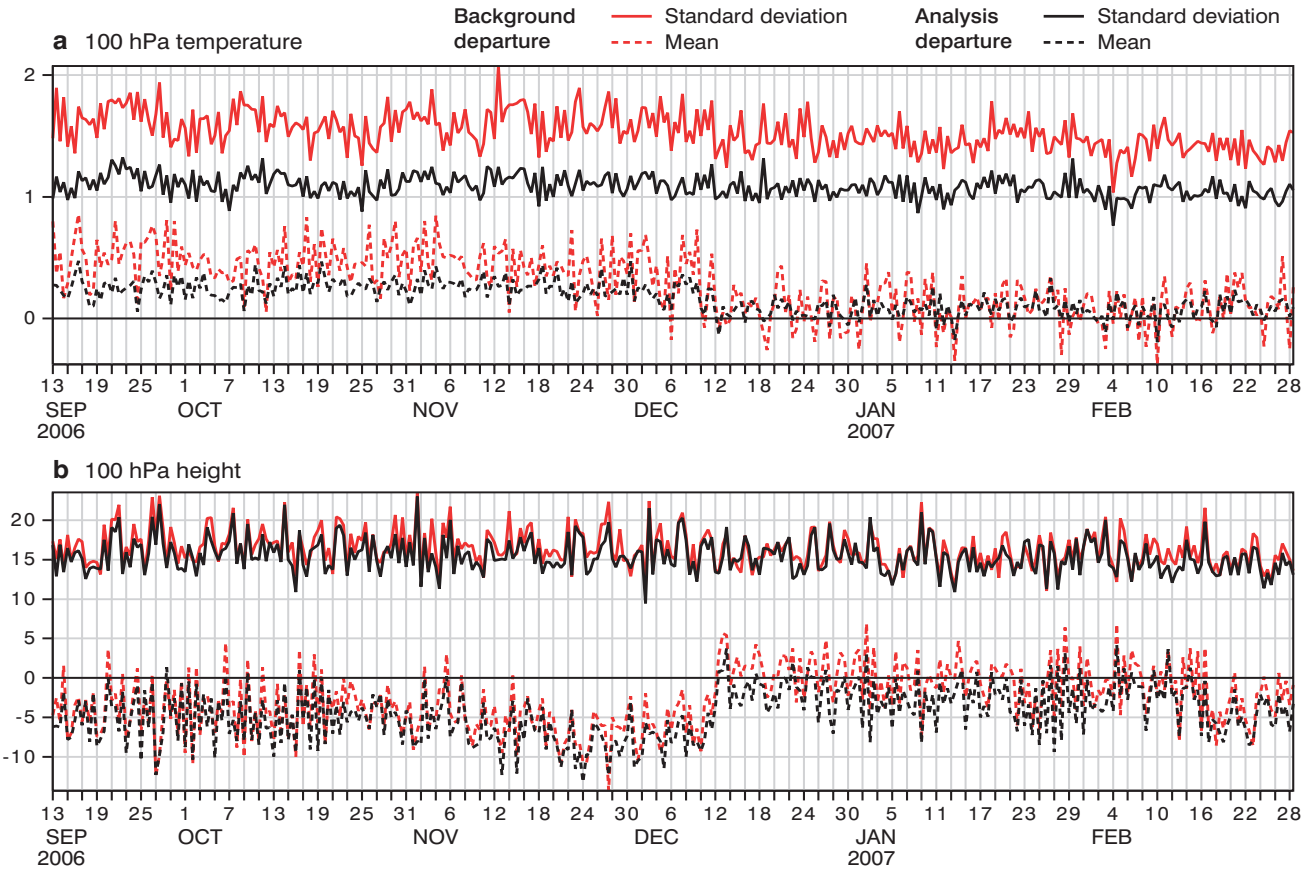

Figure 6 Time series of the mean and standard deviation of the operational background departure and analysis departure for (a) temperature and (b) height radiosonde measurements at 100 hPa. The sample numbers are typically 270 and 220 per day, for the temperature and height measurements, respectively.

Ongoing research experiments, both monitoring and assimilating the rising occultations, suggest that their error characteristics are comparable to the setting occultations, and that they contain useful atmospheric information. Therefore, it is hoped to assimilate these data operationally during 2007. In addition, in operations GPSRO measurements with tangent point within 4 km of the Earth's surface are currently not used. These measurements potentially contain useful water vapour information and their utility will be investigated further.

We will also consider the use of the two-dimensional (2D) observation operator, which accounts for the limb nature of the measurements. A 2D operator should reduce the forward model errors in the lower-troposphere, and in research experiments assimilating CHAMP measurements we have found that it has improved the fit to observations. However, the reduced forward model errors do not appear to produce improved forecasts. Nevertheless, it will be important to investigate the impact of the 2D operators now that the number of GPSRO measurements has increased by over an order of magnitude.

In the wider context, it is interesting to note that GPSRO measurements have already proved useful in research experiments investigating the assimilation AMSU-A channel 14 radiances without bias correction. It has recently been found that fixing the bias correction of AMSU-A channel 14 to zero prevents the variational bias correction scheme drifting towards the model climate in the stratosphere. However, this modification can only be done when the GPSRO measurements are assimilated, otherwise it introduces spurious temperature oscillations in the stratosphere. This is a good example of two distinct satellite observing systems complementing each other and highlights the strengths of the GPSRO measurements.

Overall, the first operational assimilation results at ECMWF suggest that GPSRO measurements are a useful addition to the global observing network. The vertical resolution of the GPSRO measurements, and the fact that they can be assimilated without bias correction, are important qualities because they mean that the measurements provide information that is complementary to the other observations. There are a number of possible improvements in the assimilation of GPSRO measurements that will be investigated soon, but it is important to emphasise that the first results at ECMWF have been very encouraging.

FURTHER READING

Anthes, **R.**, **C. Rocken** & **Y.-H. Kou**, 2000: Applications of COSMIC to meteorology and climate. *Terr. Atmos. Ocean Sci.*, **11**, 115–156.

Bormann, **N**. & **S**. **Healy**, 2005: New observations in the ECMWF assimilation system: Satellite Limb measurements. *ECMWF Newsletter No. 104*, 13–17.

Eyre, **J**., 1994: Assimilation of radio occultation measurements into a numerical weather prediction system. *ECMWF Tech. Memo. No. 199.*

Healy, **S**. & **J.-N. Thépaut**, 2006: Assimilation experiments with CHAMP GPS radio occultation measurements, *Q.J.R. Meteorol. Soc.*, **132**, 605–623.

McNally, **T**., **T. Auligné**, **D**. **Dee** & **G**. **Kelly**, 2006: A variational approach to satellite bias correction. *ECMWF Newsletter No. 107*, 18–23.

Rocken, **C.**, **R. Anthes**, **M. Exner**, **D. Hunt**, **S. Sokolovskiy**, **R. Ware**, **M. Gorbunov**, **W. Schreiner**, **D. Feng**, **B. Herman**,**Y.-H. Kuo** & **X. Zou**, 1997: Analysis and validation of GPS/ MET data in the neutral atmosphere. *J. Geophys. Res.*, **102**, 29,849–29,866.

Yunck, **T**., **C.-H**. **Lui** & **R**. **Ware**, 2000: A history of GPS sounding. *Terr. Atmos. Ocean Sci.*, **11**, 1–20.

The value of targeted observations

ROBERTO BUIZZA, CARLA CARDINALI, GRAEME KELLY, JEAN-NOËL THÉPAUT

IN THE past decade, field experiments have been organized to assess the impact of extra observations taken in some specific, case-dependent target areas identified using objective and subjective methods, on (mainly short-range) forecast accuracy. These campaigns, organized following a proposal at a workshop in 1995 (*Snyder*, 1996), were included, for example, in 1997 FASTEX (Fronts and Atlantic Storm-Track Experiment), in 1998 NORPEX (North-Pacific Experiment) and CALJET (California Land-falling JETs Experiment), in 1999 and 2000 the Winter Storm Reconnaissance Programs (WSR99 and WSR00) and in 2003 NATReC (North Atlantic THORPEX Regional Campaign). The general conclusions of these campaigns (see, e.g., *Langland*, 2005 for a review of issues in targeted observing) were that in most of the cases the impact of the targeted observations was positive, and that on average the impact was small, with maximum error reductions in some specific cases for variables such as mean-sea-level (msl) pressure of about 10–15%.

These studies were affected, by design and execution, by four major weaknesses.

- Poor matching between the target area identified by the method under investigation and the area actually sampled by the extra observations.
- Absence of a clean comparison between the impact of observations taken in objectively-defined target and randomly selected areas.
- Large variation of target areas and number of extra observations taken in the target area.
- Low statistical significance due to the limited number of cases, and biased case selection.

The study described here aims to address these four major weaknesses by comparing data-injection and data-denial experiments designed so that observations are injected or removed only in the target areas, and objectively-defined target and random areas have the same size. Furthermore, the impact of observations taken in objectively-defined target areas on downstream forecast errors, especially at forecast day 2, is analysed, and compared with observations taken in random or fixed areas with a similar size to the target areas. Finally, to be able to draw statistically significant conclusions with state-of-the-art assimilation systems, a very large number of cases (183, selected to cover different months of both warm and cold seasons) have been considered.

Data-assimilation and forecast experiments have been performed with the following version of the ECMWF system.

- Four-dimensional variational assimilation system, with a 12-hour cycling.
- Analysis resolution: outer loop $T_L511L60$, inner loops T_L159/T_L95L60.
- Forecast resolution: $T_L511L60$.

A detailed assessment of the experiments can be found in three companion papers prepared by staff at ECMWF: *Kelly et al.* (2007), *Buizza et al.* (2007) and *Cardinali et al.* (2007). Here only the key findings will be described.

Methodology and experimental design

Singular vectors (SVs) identify the perturbations growing during a finite time interval, called the optimization time interval, with the largest amplification rate measured using a defined norm (*Buizza & Palmer*, 1995). Following their successful use in the ECMWF Ensemble Prediction System, targeted SVs were used for the first time in January–February 1997 during the FASTEX field campaign (*Buizza & Montani*, 1999) to define regions where extra observations should be taken to reduce the forecast error in the verification region. Since then, SVs have been used to identify sensitive regions where targeted observations can be taken to reduce the forecast error.

Figure 1 illustrates the key concepts used in this paper to assess the value of targeted observations: T is the target area where observations should be taken to improve the day-*d* forecast inside the verification area Σ. Experiments have been run to assess the impact of ocean observations on the short-range forecast error over downstream regions (e.g. of observations located in the Pacific Ocean for forecasts verified over North America, and of observations located in the Atlantic

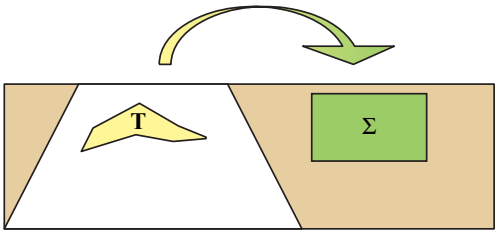

Figure 1 Schematic illustration of the concept of the 'value of targeted observations': the brown areas identify land, while the white regions identify the ocean. T is the target area (e.g. identified using singular vectors) where observations should be taken to improve the day-*d* forecast inside the verification area Σ.

Ocean for forecasts verified over Europe), and on medium-range forecast error over the whole northern hemisphere. For both sets of experiments, the ocean is defined as the area between 30°N and 80°N latitude, while the two verification regions have been defined as follows.

- European verification area: 10°W:25°E, 35°N:60°N
- North-American verification area: 125°W:90°W, 35°N:60°N

For each verification area, three types of target areas are considered.

- ***SV-target areas***: for each initial date and time (*d, h*), the SV-target area (which has always the same size) is defined using the ten leading SVs growing for two days [i.e. between (d, h) and (d+2 ,h)] with maximum final time total energy norm inside the verification region.
- ***SV-av-target areas***: for each initial date and time (*d, h*), the SV-av-target area is defined using the mean taken over the whole period under investigation of all the (*d, h*) SV-target areas (with the same size as the SV-target area).
- ***Random areas***: for each initial date and time (*d, h*), the random area has circular shape centred randomly over the ocean and with the same geographical size as the SV-target area.

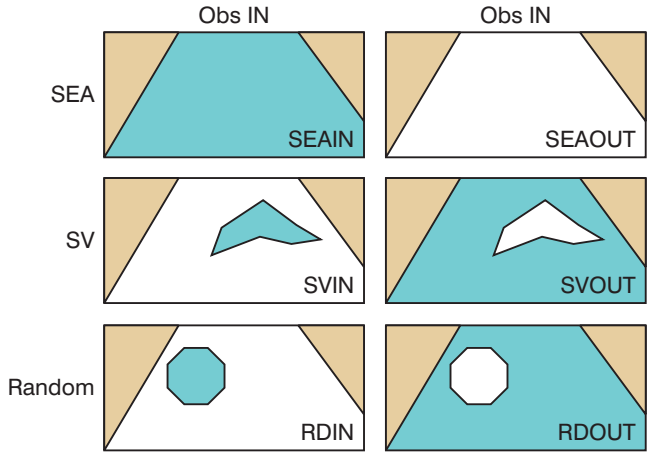

Figure 2 Schematic of the data-assimilation experiments: the brown areas identify land; the blue areas identify the areas where observations have been used, while the white areas identify the areas where observations are not used.

Figure 2 shows a schematic illustration of the six types of data-assimilations that have been performed.

- ***SEAIN***: all observations available over the ocean have been used.
- ***SEAOUT***: none of the observations available over the ocean have been used.
- ***SVIN***: only observations available in the SV-target area have been used.
- ***SVOUT***: all observations apart for the ones in the SV-target area have been used.
- ***RDIN***: only observations available in randomly defined area have been used.
- ***RDOUT***: all observations apart for the ones in randomly defined area have been used.

In experiments *SVIN* and *SVOUT*, at each data-assimilation cycle observations are either injected (*SVIN*) or removed (*SVOUT*) in the same target area defined using SVs (noting that SVs are updated every 12 hours). Similarly, in experiments *RDIN* and *RDOUT* observations are injected or removed in the same random area. For a limited subset of cases, the following experiment has also performed:

- ***SVavIN***: as *SVIN* but always using only the observations available in the SV-av-target area, defined by averaging the SV-areas computed for each day of the period under investigation.

SV-based target and random areas

The SV-based target areas have been defined, as in *Buizza & Montani* (1999), by the weighted-average (with weights defined by the singular value), vertically-integrated total energy of the SVs. For each ocean basin, the SV-target areas have been defined as the 100 grid points over the ocean with the largest value of that measure. The SVs and the corresponding target areas have been computed every 12 hours, with a configuration very similar to the one used in the ECMWF Ensemble Prediction System but with a higher resolution: T63L40 resolution, 48-hour optimization time interval, total energy norm and (dry) simplified physics. The random areas have been defined to be approximately circular, with the centre of the circle randomly selected inside the ocean region of interest, and large enough to contain the same number of grid points as the SV-target areas.

Figure 3 shows two examples of SV-target and random areas used in the Pacific-North American *SVIN* and *RDIN* experiments started at 12 UTC on 1 and 10 December 2003. In the first case, the two areas do not overlap, while in the second case the two areas have some grid points in common over the western Pacific.

Value of observations taken in the Pacific or the Atlantic Oceans

The first of the three companion papers (*Kelly et al.*, 2007) discusses the importance of data over the ocean in a mean statistical sense and for individual cases. In order to help identify 'forecast busts' a subjective method

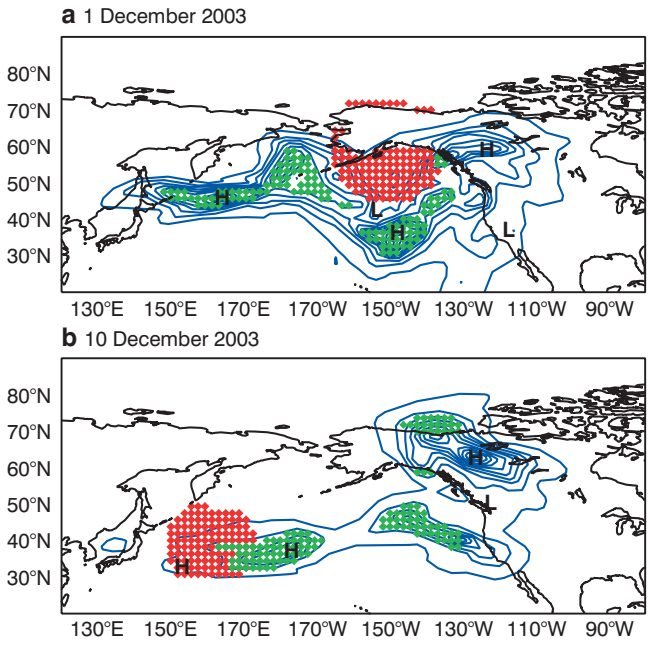

Figure 3 SV-target (green symbols) and random (red symbols) areas for the Pacific-North American region for 12 UTC on (a) 1 December and (b) 10 December 2003. The contour isolines show the weighted-average, vertically-integrated total energy of the ten leading SVs.

has been developed to find a relationship between the forecast root mean square error (rmse) and 'synoptic pattern' differences. These questions have been addressed with experiments using both three- and four-dimensional variational data-assimilation (referred to as 3D-Var and 4D-Var) performed at fairly high resolution using the ECMWF system that was operational in June 2005 for two periods: winter 2003/04 (December 2003 to February 2004, 91 days) and summer 2004 (June to August 2004, 90 days).

The key conclusions that can be drawn from the *SEAIN* and *SEAOUT* experiments are the following.

- With regard to the 4D-Var data denial experiments, the data from the Pacific is more important to reduce the two-day forecast error over North America (Figure 4) than the corresponding Atlantic oceanic data to reduce the two-day forecast error over Europe (Figure 5), although both denial experiments clearly show a downstream forecast degradation. The comparison of 4D-Var and 3D-Var experiments has indicated that removing oceanic data has a larger impact on downstream forecast accuracy if a 3D-Var assimilation system is used.
- In the 4D-Var system the influence of observations remains fairly local and mainly affects the immediate downstream region throughout the whole ten-day forecast range (Figure 6). In particular, on average there is a very little impact of removing observations in the Pacific on medium-range forecasts over Europe during winter (Figure 4), while the impact in summer is slightly larger (not shown, for further details see *Kelly et al.*, 2007). Similarly, removing observations in the Atlantic does not affect forecasts for the Pacific-North American region. Again, the comparison of 4D-Var and 3D-Var experiments indicates that the impact of removing oceanic observation is less local if a 3D-Var assimilation system is used.

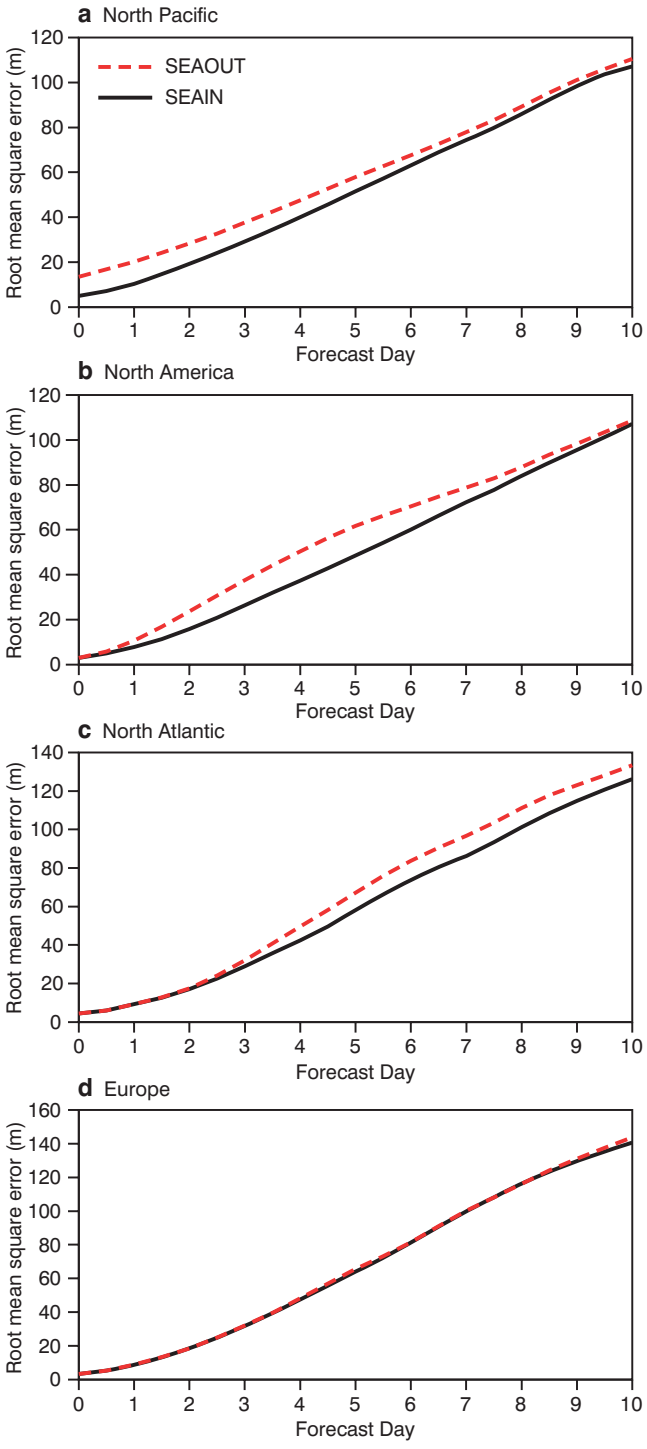

Figure 4 The rmse of mean 500 hPa geopotential height for up to day ten for *SEAOUT* and *SEAIN* for winter Pacific forecasts. Both experiments are verified using the ECMWF operational analysis. Verification regions are (a) North Pacific, (b) North America, (c) North Atlantic and (d) Europe (panels are ordered to reflect the downstream propagation of the impact of removing observations, starting from the North Pacific).

- In a few, selected cases the impact of removing oceanic data can be very large and detectable on 500 hPa geopotential synoptic maps. In particular, a detailed synoptic evaluation performed for the Atlantic-European region has indicated that large synoptic differences between the 48-hour forecasts of *SEAIN* (the experiment using all oceanic data) and *SEAOUT* (the experiment removing all oceanic data over the Atlantic) could lead to forecast rmse differences of more than 15 m at 500 hPa at day 2 in a small number of cases (16% in winter and 14% in summer). The Pacific *SEAOUT* experiments have a much larger effect than the Atlantic ones. The impact remains relatively small in summer.

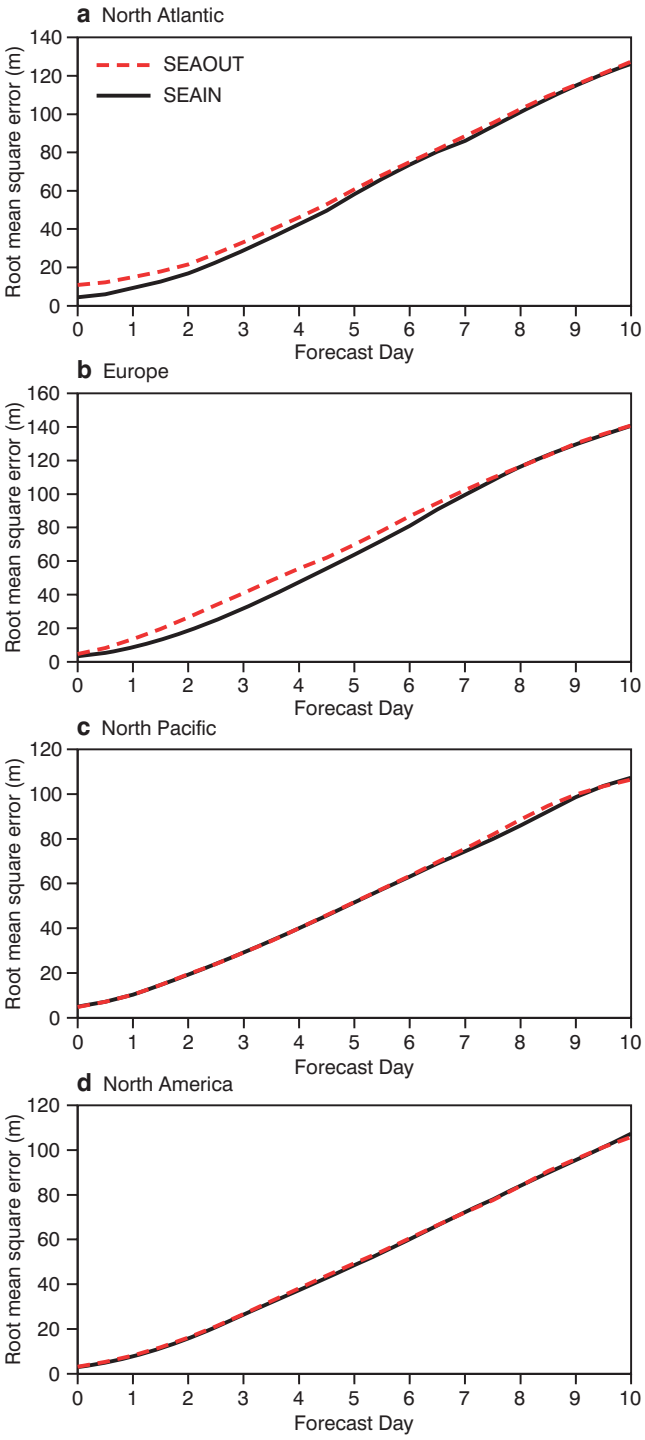

Figure 5 The rmse of mean 500 hPa geopotential height for up to day ten for *SEAOUT* and *SEAIN* for winter Atlantic forecasts. Both experiments are verified using the ECMWF operational analysis. Verification regions are (a) North Atlantic, (b) Europe, (c) North Pacific and (d) North America (panels are ordered to reflect the downstream propagation of the impact of removing observations, starting from the North Atlantic).

The fact that denying observations in 3D-Var has a larger impact than in 4D-Var should be interpreted with care. Figure 7 displays an idealistic representation of the analysis accuracy as a function of the number of observations (all units and numbers are arbitrary). 4D-Var and 3D-Var should give the same results in terms of analysis accuracy when there are no observations and when there are infinitely many observations (the assimilation system should not matter anymore if infinite observations are assimilated). The experience, backed up by many impact studies performed in the past, suggests that the analysis improvement in case of 4D-Var is likely to follow the blue curve, while a less performing system (e.g. 3D-Var) will follow the red curve.

Figure 7 shows that going for example from 0 to 25 observations will lead to a 0.26 improvement in 3D-Var (red vertical bar) against 0.39 (blue dotted vertical bar) in 4D-Var. It has indeed been demonstrated and documented in *Thépaut* (2006) that in the sole presence of surface pressure observations, 4D-Var was outstandingly better than 3D-Var, indicating a much sharper curve (analysis improvement as a function of number of observation) in a data void context. The experiments reported here are performed in a system overwhelmed by observations (in particular satellite data), which probably corresponds to a regime of around 150 observations in the idealistic context. Although 4D-Var is clearly better than 3D-Var in our experimental framework, the incremental gain (loss) achieved by adding (denying) an overall limited number of observations will be higher in 3D-Var than in 4D-Var (red and blue vertical bars around 150 observations: increment of 0.017 for 4D-Var against 0.048 for 3D-Var).

Value of observations in SV-based target areas

The second of the three companion papers (*Buizza et al.*, 2007) discusses some fundamental questions about the value of targeted adaptive observations: what is the 'value' of observations taken in target regions identified using SVs compared to the value of observations taken in randomly chosen regions? Is it important that SV-target regions are identified using the most recent analysis and forecast, or can an SV-av-target region be used? Does the 'value' of observations depend on the region?

Figure 8 compares the average rmse of *SVIN*, *SVavIN* and *RDIN* with the two reference forecasts *SEAOUT* and *SEAIN* for both the Pacific and Atlantic experiments. Similarly, Figure 9 compares the average rmse of *SVOUT* and *RDOUT* with the two reference forecasts

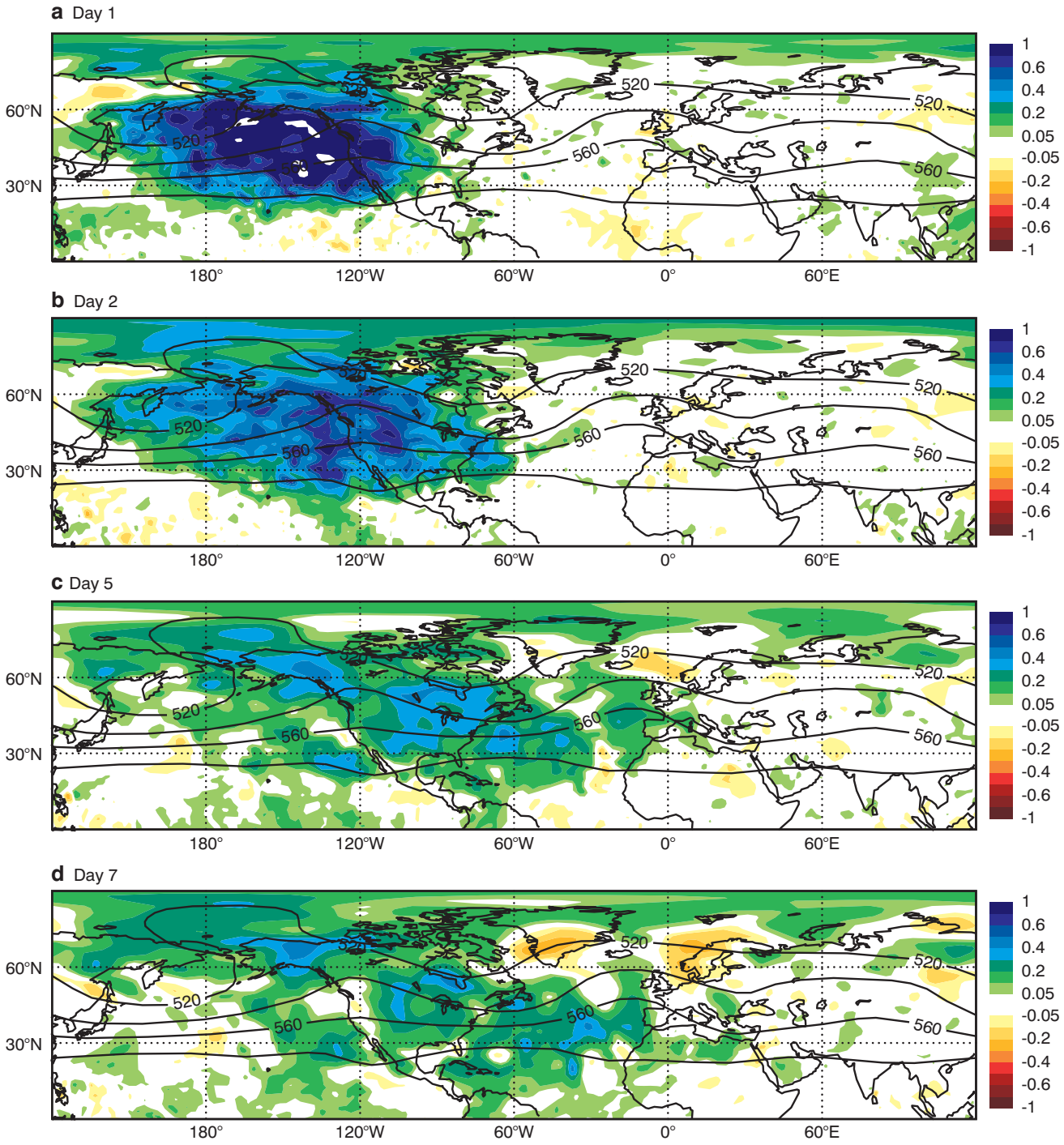

Figure 6 Normalized rmse differences between *SEAIN* and *SEAOUT* for winter Pacific forecasts for (a) day 1, (b) day 2, (c) day 5 and (d) day 7. Blue-purple show the negative impact and yellow-black the positive impact of *SEAOUT*.

for the two regions. The following three general conclusions can be drawn from the comparison of forecasts started from the seven types of experiments run for winter 2003/04 and summer 2004.

- Observations taken in SV-target areas are more valuable than observations taken in random areas, with the difference depending on the region, the season and the baseline observing system used as a reference.
- It is important that the daily set of singular vectors is used to compute the target areas. Experiments run for the Pacific-North American region for winter 2003/04 indicated that observations taken in a fixed target area identified considering the average of all the daily SV-target areas would have a smaller value than observations taken in the daily SV-target areas (while *SVIN* experiments have an average a 27.5% smaller error than *SEAOUT*, *SVavIN* experiments have a 20.9% smaller error, see Table 1). However, this would have to be mitigated against the cost of deploying a daily targeting strategy.
- The value of observations taken in SV-target areas defined using SVs optimized for a two-day period

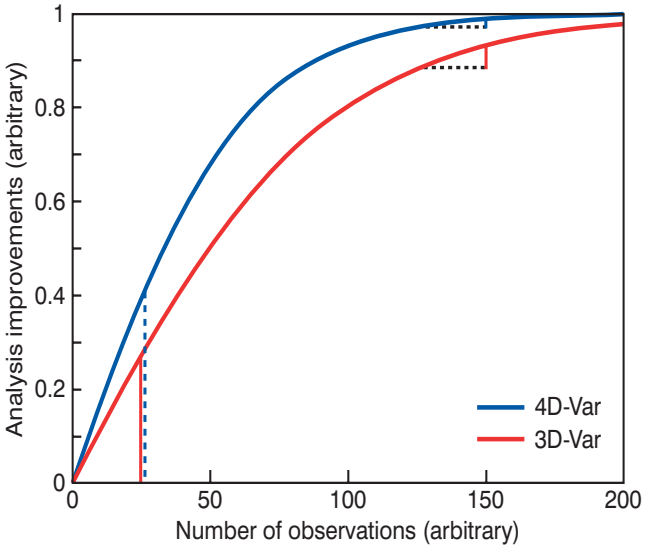

Figure 7 Idealistic representation of the analysis improvement as a function of the number of assimilated observations (numbers and units are arbitrary) for 4D-Var and 3D-Var. The vertical full red bars represent the improvement of the 3D-Var analysis when one goes from zero to 25 observations, and from 125 to 150 observations. The vertical dotted blue bars represent the same quantities for 4D-Var.

starts decreasing after forecast day 3 because the impact of the targeted observations moves outside the verification region after that time.

In particular, results have indicated that:

- *If the baseline observing system is data void (i.e. no observations) over the ocean, then the average value of observations taken in SV-target areas is fairly high.* Consider the value measured using the rmse of 500 hPa geopotential height forecasts (Tables 1 and 2). These results indicate, for example, that SV-targeted observations are capable of reducing the two-day average forecast error in the verification region by 27.5% in winter 2003/04 for SV-targeted Pacific observations with forecasts verified over North America (compared to 15.7% for randomly targeted observations); this corresponds to 13.5 hours of forecast gain.
- *If the baseline observing system is data rich (i.e. with all observations) over the ocean, then the average value of observations taken in SV-target areas is very small.* In terms of the rmse of the 500 hPa geopotential height forecasts, the results indicate, for example, that removing SV-targeted observations increases the two-day average forecasts error in the verification region by

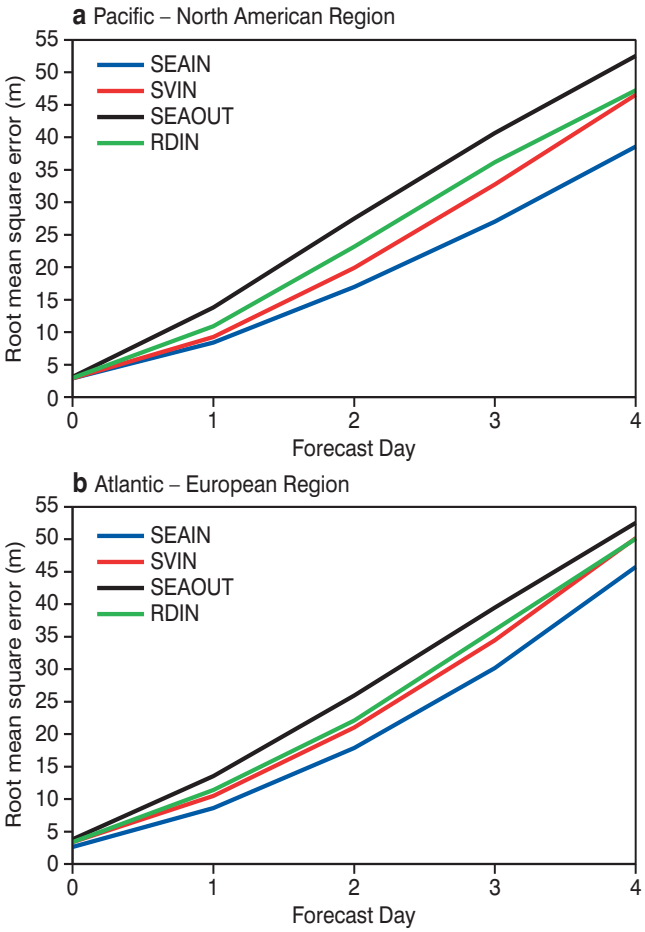

Figure 8 Average rmse of 500 hPa geopotential height forecasts of experiments *SEAIN*, *SEAOUT*, *SVIN* and *RDIN* run for (a) Pacific-North American region and (b) Atlantic–European region for winter 2003/04.

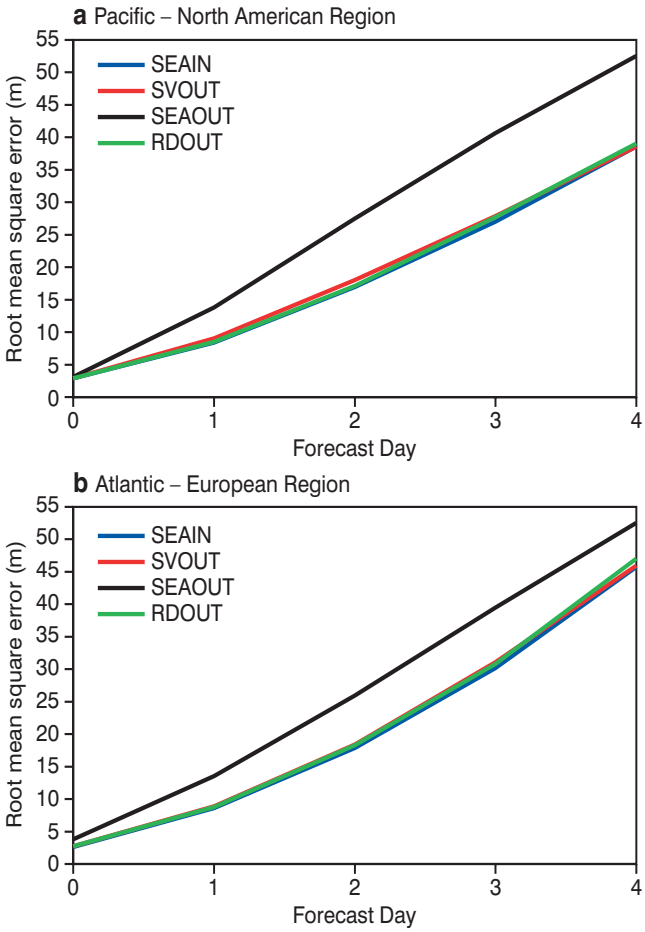

Figure 9 Average rmse of 500 hPa geopotential height forecasts of experiments *SEAIN*, *SEAOUT*, *SVOUT* and *RDOUT* run for (a) Pacific-North American region and (b) Atlantic–European region for winter 2003/04.

Experiment	Root mean square error (rmse)	
	Winter 2003/04	Summer 2004
SEAOUT	27.49 m	16.57 m
SEAIN	16.96 m	11.96 m
SVIN	19.93 m	13.90 m
RDIN	23.18 m	14.61 m
SVOUT	18.06 m	12.20 m
RDOUT	17.11 m	11.81 m
SVavIN	21.75 m	–
Measure of impact	**Normalised rmse differences (predictability gain)**	
	Winter 2003/04	**Summer 2004**
(SEAIN-SEAOUT) / SEAOUT	38.3% (18.8 h)	27.8% (13.5 h)
(SVIN-SEAOUT) / SEAOUT	27.5% (13.5 h)	16.0% (7.8 h)
(RDIN-SEAOUT) / SEAOUT	15.7% (7.7 h)	11.8% (5.7 h)
(SVavIN-SEAOUT) / SEAOUT	20.9% (10.3 h)	–
(SEAIN-SVOUT) / SEAOUT	4.0% (2.0 h)	1.3% (0.7 h)
(SEAIN-RDOUT) / SEAOUT	0.5% (0.3 h)	-1.1% (-0.4 h)
(SVOUT-SEAIN) / SEAIN	6.5%	2%
(RDOUT-SEAIN) / SEAIN	0.9%	-1.5%

Table 1 Average value of observations taken in different target areas, measured using the rmse of the two-day forecasts of 500 hPa geopotential height over North America. The upper part of the table gives the rmse (metres) of the forecast experiments. The lower part shows the normalized differences in rmse (percent) between pairs of experiments, with the normalization done using the rmse of the *SEAOUT* experiment for all but the last two rows where the rmse of *SEAIN* has been used. The corresponding change in predictability in hours is given in brackets.

Experiment	Root mean square error (rmse)	
	Winter 2003/04	Summer 2004
SEAOUT	25.98 m	17.96 m
SEAIN	17.87 m	10.25 m
SVIN	21.02 m	12.82 m
RDIN	22.10 m	13.04 m
SVOUT	18.40 m	10.62 m
RDOUT	18.33 m	10.40 m
SVavIN	–	–
Winter 2003/04	**Normalised rmse differences (predictability gain)**	
	Winter 2003/04	**Summer 2004**
(SEAIN-SEAOUT) / SEAOUT	31.2% (15.0 h)	42.9% (21.7 h)
(SVIN-SEAOUT) / SEAOUT	19.1% (9.2 h)	28.6% (14.5 h)
(RDIN-SEAOUT) / SEAOUT	14.9% (7.2 h)	27.3% (13.8 h)
(SVavIN-SEAOUT) / SEAOUT	–	–
(SEAIN-SVOUT) / SEAOUT	2.0% (1.0 h)	2.1% (1.0 h)
(SEAIN-RDOUT) / SEAOUT]	1.7% (0.8 h)	0.8% (0.4 h)
(SVOUT-SEAIN) / SEAIN	3.0%	3.6%
(RDOUT-SEAIN) / SEAIN	2.6%	1.6%

Table 2 Average value of observations taken in different target areas, measured using the rmse of the two-day forecasts of 500 hPa geopotential height over Europe. The upper part of the table gives the rmse (metres) of the forecasts experiments. The lower part shows the normalised differences, in percent, between pairs of experiments, with the normalization done using the rmse of the *SEAOUT* experiment for all but the last two rows where the rmse of *SEAIN* has been used. The corresponding change in predictability in hours is given in brackets.

4.0% in winter 2003/04 for SV-targeted Pacific observations and forecasts verified over North America (compared to 0.5% for randomly targeted observations); this corresponds to two hours of forecast gain. The data-denial experiments do not replicate precisely the impact that adding extra observations taken in targeted regions may have on forecast accuracy, but in our view they can be used to estimate the potential average impact that they may have. In the (strong) hypothesis that the characteristics (type, quality, content of information) of future extra observations is similar to the characteristics of the observations removed, the data-denial experiments provide an upper bound of the expected average impact that extra observations may have.

The fact that, for the Pacific, the value of observations taken in SV-target is smaller in summer, and the difference between the value of observations taken in the SV-target versus random areas is also smaller in summer, is possibly due to the characteristics of the SVs (*Buizza & Palmer*, 1995). In winter, the amplification rate spectrum of SVs is steeper, which makes it easier to separate the leading ten from the others, in particular from the directions spanned by the random area. Furthermore, in winter the SVs are more localized in the storm track region, again making their location more 'different' from the location identified by the random areas. Finally, it is worth remembering that the SVs have been computed with a simplified, dry tangent forward and adjoint physics, which may make their computation less accurate in summer, a period during which moist processes play a bigger role than in winter.

These values could be compared to the reduction of the 48-hour forecast error of the ECMWF high-resolution forecast between 1995 and 2005: over North

America, the rmse of the 500 hPa geopotential height was reduced from about 25 to 16 m (i.e. by ~36%), while over Europe the rmse was reduced from about 24 to 15 m (i.e. by ~37%). In other words, development of the observation network and ECMWF data assimilation and forecasting system led to a forecast error reduction of about 3.6–3.7% per annum. *Thus, the average impact of SV-targeted observations in the case of a data-rich baseline observing system over the ocean is comparable to the annual forecast error reduction of the ECMWF high-resolution forecast.*

Weather regime sensitivity of the value of targeted observations

The third of the three companion papers (*Cardinali et al.*, 2007) discusses the sensitivity to the atmospheric flow of targeted observations taken in the Atlantic for forecasts verified over Europe. Four different periods characterized by different large-scale circulation during the tropical cyclones season have been examined: A02 (26 July to 16 August 2002), S03 (1 to 23 September 2003), A05 (13 to 21 August 2005) and S05 (4 to 27 September 2005). Results based on *SEAIN*, *SEAOUT*, *SVOUT* and *RDOUT* experiments for these four periods indicate the following.

- The value of targeted observations is sensitive to the interaction of tropical disturbances with the mid-latitude flow, with targeted observations capable of reducing the forecast error by up to 13%, when error is measured in terms of averaged rmse of the 500 hPa geopotential height over the verification area.
- SV-based targeted observations in sensitive regions of North America computed by using energy norm and dry singular vectors are on average six times more valuable than a target randomly selected areas over the ocean.

The maximum forecast response to targeted observations is detected when extra-tropical transitions take place and the large-scale flow over the Atlantic is non-zonal and rather unstable. It should be also kept in mind that a rmse reduction smaller than 15 m (~40%) does not generally bring substantial synoptic forecast differences at tropospheric levels but can provide some significant changes to the surface pressure field as was shown for August 2002 and 2005 (see *Kelly et al.*, 2007).

Sensitivity regions are believed to indicate dynamically active regions which are very important to identify. Denying observations in sensitive areas is therefore expected to produce a larger loss of information content than in random areas, being the maximum effect when full flow-dependent structure functions are used. Anyhow, the observation departures propagated back in time by the adjoint model to the beginning of the assimilation window do provide a similar effect in the covariance evolution. Also a larger observation influence

Cases	Degradation Relative to SEAIN (%)			Absolute Forecast Error (m)		
	(SVOUT–SEAIN)/SEAIN	(RDOUT–SEAIN)/SEAIN	(SVOUT–RDOUT)/SEAIN	SVOUT	RDOUT	SEAIN
Extra-tropical cases						
August 2002 8 day	8.1	1.4	6.7	13.0	12.1	12.0
September 2003 4 day	6.0	-3.9	9.9	17.3	15.7	16.4
August 2005 8 day	12.9	2.1	10.8	11.6	10.5	10.2
September 2005 23 day	3.3	1.5	1.8	11.6	11.4	11.2
All cases						
2002 21 day	4.5	2.5	2	12.8	12.5	12.2
2003 21 day	1.5	-2.7	4.2	13.7	13.1	13.5
2005 57 day	3.9	2.0	1.9	11.4	11.2	11.0
Seasons						
Summer 2004 90 day	3.6	1.6	2.0	10.6	10.4	10.2
Winter 2003/04 90 day	3	2.6	0.4	18.4	18.3	17.9

Table 3 Average rmse over Europe for the two-day forecasts of 500 hPa geopotential height computed for the extra-tropical cases analyzed in *Cardinali et al.* (2007), all cases discussed in the three companion papers, and the two seasons discussed in *Buizza et al.* (2007). The first three columns give the percentage of degradation relative to *SEAIN* of *SVOUT*, *RDOUT* and (*SVOUT–RDOUT*) and the last three columns the absolute forecast error in metres are averaged over Europe.

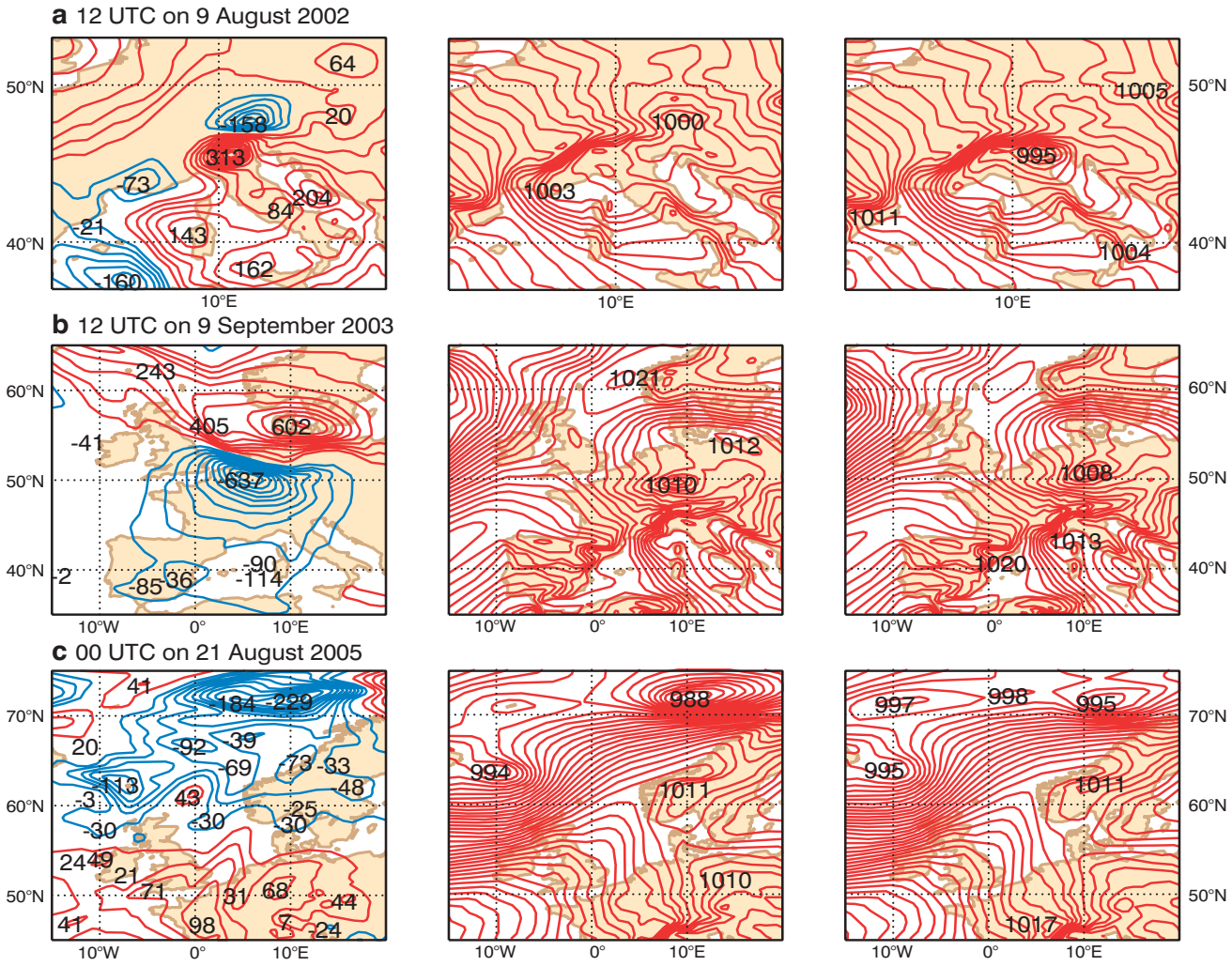

Figure 10 48-hour forecast of the 500-hPa geopotential height differences between *SVOUT* and *RDOUT* (first column), msl pressure for *SVOUT* (second column), and msl pressure for *RDOUT* (third column) valid at (a) 12 UTC on 9 August 2002, (b) 00 UTC on 9 September 2003 and (c) 00 UTC on 21 August 2005.

loss is observed in all experiments where data has been denied in sensitive areas. While examining the short-range forecast, it has been noticed that 12-hour geopotential height forecast error measured over the Atlantic, which includes both sensitive and random regions where data were denied, is larger for those experiments where observations are missing in sensitive regions. Poorer first-guest fields are clearly determined by the poorer analysis quality.

Overall, this study validates and confirms the hypothesis on which targeting of sensitivity regions are based. Table 3 shows that, although on average over many cases the impact of SV-based targeted observations on two-day forecast of 500 hPa geopotential height is 3.3%, in selected cases of extra-tropical transitions the value increases to be 12.9%. Figure 10 shows three cases with large rmse degradation and significant changes in the surface fields.

Figure 10(a) shows, from left to right, the 48-hour 500 hPa forecast differences between *SVOUT* and *RDOUT*, the msl pressure for *SVOUT*, and msl pressure for *RDOUT* valid at 12 UTC on 11 August 2002. At 500 hPa the differences of 31 m are due to a stronger intensification and time shifting of the low system, amplified by the interaction with Tropical Cyclone Cristobal; the msl pressure in *SVOUT* presents a minimum of 1000 hPa whilst in *RDOUT* it is 995 hPa. Rejecting observations in a sensitive area causes a disruption of the surface pressure field whilst *RDOUT* surface field stays similar to *SEAIN* (not shown). This period was characterized by heavy precipitation with flooding in parts of Central Europe. The accumulated forecast precipitation over 48 hour from 00 UTC on 9 September for *SVOUT* and *RDOUT* shows very different patterns but similar intensities (not shown).

Figure 10(b) depicts a case valid at 00 UTC on 11 September 2003 (forecast started at 00 UTC on 9 September) during the Fabian extra-tropical transition. Removing observations in sensitive areas first lessens the low pressure system (moving northwards) northwest of England by 6 hPa (not shown) and 12 hours later some changes occur in the displacement and intensity of the low pressure system over Germany (second and third columns, respectively).

Figure 10(c) is related to the Irene transition into the extra-tropical flow. Large differences are observed north of Scandinavia in the msl pressure fields between *SVOUT* and *RDOUT* (not included in the rmse verification region) with a 7 hPa maximum difference. This time, denying observations in a sensitive region creates a surface pressure system which is too deep. On average for all periods, differences of 20 m are observed in the troposphere and sometimes there are corresponding significant changes to the pressure distribution at the surface.

Target field campaigns tend to investigate the impact on forecasts of extreme weather events (that very often do not occur). Also the size of the target and verification area change at every observational campaign. The results presented here suggest that it would be preferable to target more continuously during specific weather situations as, for example, extra-tropical cyclone transitions.

A framework to investigate the value of targeted observations

This study has provided an updated estimate of the potential value of targeted observations. In addition it proposes a framework that could be applied to (a) study the value of other objective targeting methodologies and (b) investigate their sensitivity to the data-assimilation system used to assimilate the extra observations. In particular, this framework could be used:

- To investigate whether using moist SVs would increase the value of observations taken in SV-target areas, and increase the difference between the value of observations taken in SV-target and random areas in the summer.
- To study the sensitivity of the value of targeted observations taken over land from higher quality observation platforms, capable to provide more accurate data both in cloud-free and cloud-covered areas. High quality data in the right place could have a non-negligible impact. However, such experiments, if they were to show too little impact, could be criticized as being unrepresentative on the grounds that observation removal is taking place over regions where error growth characteristics are rather different than those over the oceanic storm track.
- To compare the value of observations taken in SV-based target regions with observations taken in areas objectively identified using other methodologies (*Majumdar et al.*, 2006) so as to assess whether these other methodologies can lead to a better use of targeted observations.
- To further assess the forecast degradation caused by data-denial in target areas during other cases of extra-tropical cyclone transitions.

One of the interesting outcomes of this study is the local nature of data denial when 4D-Var is used to assimilate the data. The propagation of the analysis error downstream reduces rapidly, and little effect on any European forecasts was detected from the Pacific denial experiments. This result is an indication of the superiority of 4D-Var over the previous 3D-Var assimilation system, and a proof of its robustness and capacity to compensate for the lack of accurate observations.

FURTHER READING

Buizza, **R**. & **T.N**. **Palmer**, 1995: The singular-vector structure of the atmospheric global circulation. *J. Atmos. Sci.*, **52**, 1434–1456.

Buizza, **R**. & **A**. **Montani**, 1999: Targeting observations using singular vectors. *J. Atmos. Sci.*, **56**, 2965–2985.

Buizza, **R.**, **C**. **Cardinali**, **G**. **Kelly** & **J.-N**. **Thépaut**, 2007: The value of targeted observations Part II: the value of observations taken in singular vectors-based target areas. *ECMWF Tech. Memo. No. 512* (submitted to the *Q. J. R. Meteorol. Soc.*).

Cardinali, **C**. & **R**. **Buizza**, 2003: Forecast skill of targeted observations: a singular-vector-based diagnostic. *J. Atmos. Sci.*, **60**, 1927–1940.

Cardinali, **C.**, **S**. **Pezzulli** & **E. Andersson**, 2005: Influence-matrix diagnostic of a data assimilation system. *Q. J. R. Meteorol. Soc.*, **130**, 2767–2786.

Cardinali, **C.**, **R**. **Buizza**, **G**. **Kelly**, **M**. **Shapiro** & **J.-N**. **Thépaut**, 2007: The value of targeted observations Part III: weather regimes influence. *ECMWF Tech. Memo. No. 513* (submitted to the *Q. J. R. Meteorol. Soc.*).

Kelly, **G.** 1997: Influence of observations on the operational ECMWF system. *WMO Bulletin*, **46**, 336–341.

Kelly, **G.**, **A**. **McNally**, **J.-N**. **Thépaut** & **M**. **Szyndel**, 2004. Observing System Experiments of all main data types in the ECMWF operational system. In *Proc. of the Third WMO Workshop on the Impact of Various Observing Systems on NWP Alpbach, Austria, 9–12 March 2004.*

Kelly, **G.**, **J.-N**. **Thépaut**, **R**. **Buizza**, & **C**. **Cardinali**, 2007: The value of targeted observations Part I: data denial experiments for the Atlantic and the Pacific. *ECMWF Tech. Memo. No. 511* (submitted to the *Q. J. R. Meteorol. Soc.*).

Langland, **R.H**., 2005: Issues in targeted observing. *Q. J. R. Meteorol. Soc.*, **613**, 3409–3425.

Majumdar, **S.J**., **S.D**. **Aberson**, **C.H**. **Bishop**, **R**. **Buizza**, **M**. **Peng** & **C**. **Reynolds**, 2006: A comparison of adaptive observing guidance for Atlantic tropical cyclones. *Mon. Wea. Review*, **134**, 2354–2372.

Snyder, **C**., 1996: Summary of an informal workshop on adaptive observations and FASTEX. *Bull. Amer. Meteorol. Soc.*, **77**, 953–961.

Thépaut, **J.-N**., 2006: Assimilating only surface pressure observations in 3D and 4D-Var. In *Proc. of the ECMWF/GEO Workshop on Atmospheric Re-analysis*, ECMWF, 19–22 June 2006.

Ensemble streamflow forecasts over France

FABIENNE ROUSSET REGIMBEAU, FLORENCE HABETS, ERIC MARTIN, JOËL NOILHAN

IN RESPONSE to the increasing need for a better anticipation of severe hydrological events, the use of ensemble forecasts in hydrology is emerging as a key activity within the international scientific community. In 2004, a new international project was started, the Hydrological Ensemble Prediction Experiment (HEPEX), which brings together hydrological and meteorological communities to build a research project focused on advancing probabilistic hydrologic forecast techniques. This involves efforts on how to produce, disseminate, use and verify ensemble hydrological forecasts. Within the framework of HEPEX, inter-comparison experiments have been organized. Another European effort using hydrological ensemble forecasts is the development of the European Flood Alert System (EFAS) supported by the European Commission. The aim is to provide a harmonized Europe-wide long-term flood alert system in cooperation with national operational flood-forecasting centres. In addition to these international actions, the coupled hydrometeorological model SIM (SAFRAN-ISBA-MODCOU), developed for several years at Météo-France, is now the basis of on an ensemble streamflow forecast system.

The ensemble streamflow prediction system based on SIM has been running in real-time since 4 September 2004. It is forced by the ten-day meteorological ensemble forecasts from ECMWF. These forecasts are downscaled to the resolution of ISBA, which runs on a regular 8 km grid. A statistical analysis of the skill of the system was performed over nearly one year, using standard metrics for ensemble forecasts (e.g. Brier Score, Ranked Probability Score and Talagrand Histograms). It showed overall good results, for high flows as well as for low flows. In addition, a study of a few significant flood events from the past reveals that ensemble forecasts can be of great use to hydrological forecasters.

The SIM system

The SIM system is composed of a meteorological analysis system (SAFRAN), a land surface model (ISBA) and a hydrogeological model (MODCOU). It was first used in a forced mode in which the atmospheric forcing was derived from observations using SAFRAN. It has been validated over the long term for three large (regional scale) French basins and then for the whole of France. It has been shown that SIM is capable of reproducing the water and energy budgets, as well as the observed streamflows, aquifer levels and snow pack, particularly for basins with areas of over 1000 km2. In a recent study of the Seine basin, it was shown that the ability of SIM to reproduce the evolution of the aquifers and the partitioning between surface runoff and drainage leads to a good simulation of the main flood events of the Seine. Since 2003, the SAFRAN and ISBA modules have been used in an operational analysis mode at Météo-France, while the MODCOU module has been used in an experimental real-time analysis mode. This system provides a daily monitoring of the components of the water budget (such as soil moisture, snow pack, aquifer and river levels) over all France.

The real time ensemble streamflow prediction (ESP) system

The ensemble streamflow prediction (ESP) system developed at Météo-France is based on the SIM system. The idea is to use the ten-day ensemble forecasts from ECMWF instead of the SAFRAN analysis. An important goal of this ensemble prediction system is the ability to forecast the streamflow of large French basins, such as the Seine, and in particular the long-duration floods of these basins. The ensemble forecasts also provide valuable information during low flow periods, in which case the hydrographic system responses are strongly deter-

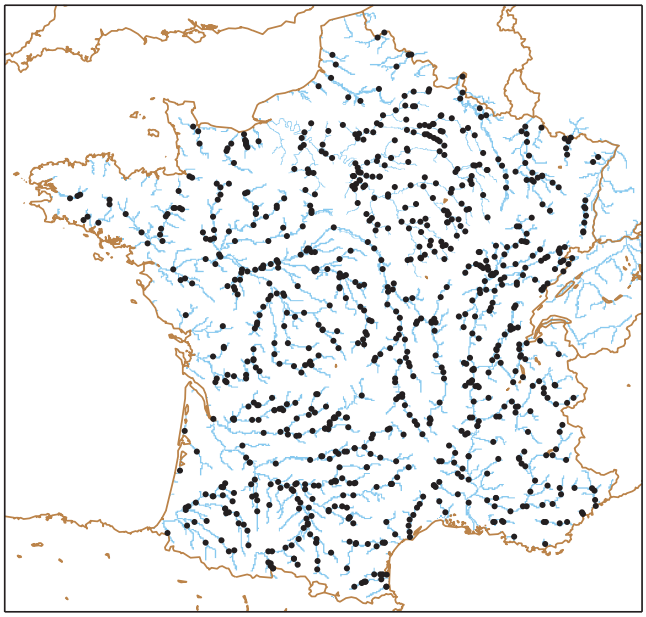

Figure 1 French hydrographic network used in SIM, and the position of the 900 river gauging stations over France.

AFFILIATIONS

Fabienne Rousset Regimbeau, **Eric Martin**, **Joël Noilhan**: CNRM Météo-France, 42 avenue Coriolis, 31057 Toulouse, France

Florence Habets: CNRS, UMR-SISYPHE, ENSMP, 35 rue St Honoré, 77305 Fontainebleau, France

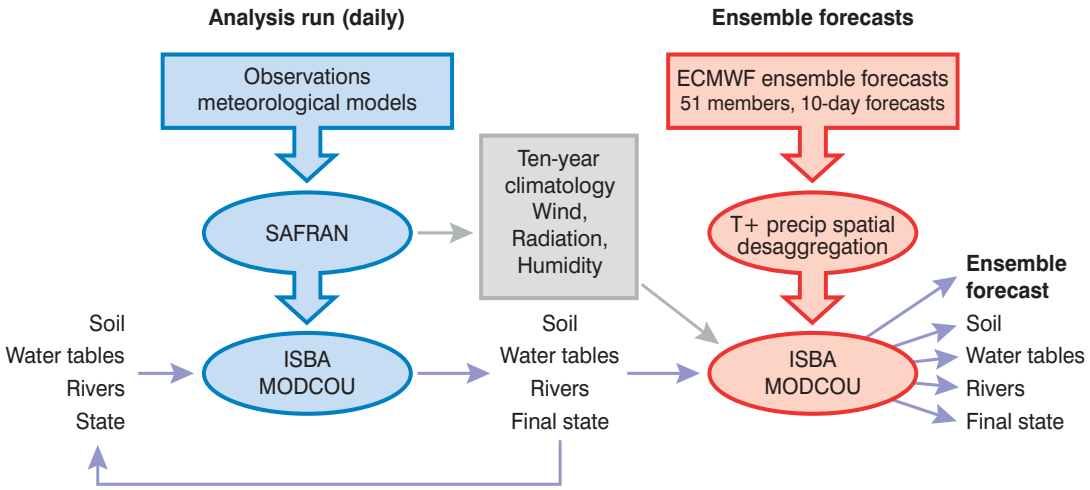

Figure 2 Schematic of the SIM hydrometeorological coupled system (left) and of the ensemble streamflow prediction system based on SIM (right).

mined by the aquifers. The ten-day lead time of these ensemble forecasts is a major advantage: it provides information at a significant lead time. Such a lead time is not possible using the classical method, which consists in obtaining a several-day streamflow forecast from time extrapolation of the observed upstream flows.

The ten-day 51-member ensemble forecasts from ECMWF are used as an input of the ISBA and MODCOU modules, which produce 51 ten-day streamflow forecasts for about 900 river gauges over France (Figure 1). The initial conditions are provided by the real time SIM analysis. In particular, the soil wetness, the aquifer level and the amount of water stored in the rivers are initialised according to the real-time monitoring. The 00 UTC ECMWF ensemble forecasts are available daily in the Météo-France database, at a 1.5° resolution, with a 6-hour time step. In order to reduce the costs of calculation time and memory space, two adaptations were made.

- It was shown that the time step of ISBA could be increased from 5 minutes to 20 minutes without significantly changing the results (regarding the streamflows).
- It was determined that we only needed to use the ensemble forecasts of precipitation and temperature, while a climatology (based on the SAFRAN analysis, 1995–2003 mean) could be used for the other meteorological parameters used by ISBA.

A schematic of the SIM hydrometeorological coupled system and of the ensemble streamflow prediction system based on SIM is shown in Figure 2.

Moreover, a spatial downscaling method was set up in order to adapt the 1.5° ensemble forecasts from ECMWF (temperature and precipitations) to the 8 km ISBA grid. We chose a simple method, based on that used by the SAFRAN analysis system, in order to maintain coherence between the operationally analysed SAFRAN and the ensemble forecasts. Figure 3 shows an example of this downscaling for one particular forecast period, with a map of the ECMWF data (Figure 3(a)) and a map of the data downscaled on the ISBA 8 km grid (Figure3(b)).

The downscaling is computed in two steps and uses an intermediate grid which consists of the SAFRAN zones (615 non regular zones, about 20×20 km each).

- Data from ECMWF is interpolated horizontally onto the SAFRAN zones using distance-dependent weights ($1/r^2$ interpolation).
- Altitude effects are then taken into account by imposing a vertical gradient within each zone which is computed as the difference between the ECMWF and ISBA grid-box average altitudes.

The vertical gradients are nearly the same as in SAFRAN: for the forecast temperature we use the ICAO gradient (-0.65 K/100 m), and for the forecast precipitation the value of the gradient is close to the one generally used

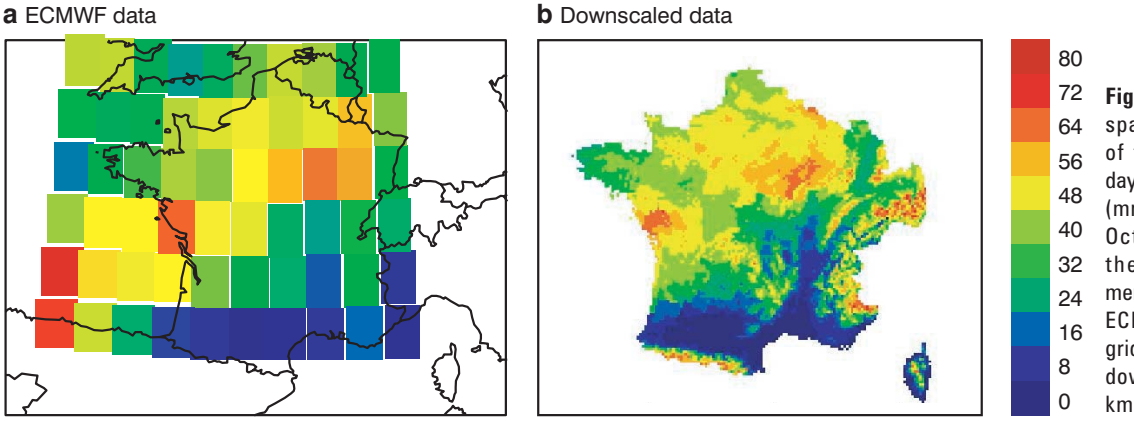

Figure 3 Result of the spatial downscaling of the ECMWF ten-day cumulative rainfall (mm), forecast for 17 October 2004, from the first ensemble member: (a) data from ECMWF on the 1.5° grid and (b) data after downscaling on the 8 km grid.

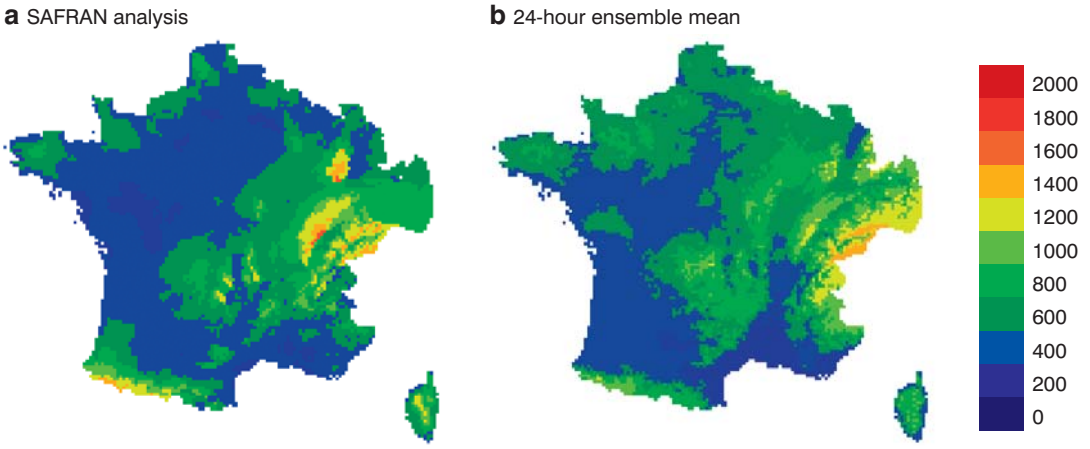

Figure 4 Result of the spatial downscaling of ECMWF cumulative rainfall (mm) from 4 September 2004 to 31 July 2005: (a) SAFRAN observation analysis and (b) 24-hour ensemble mean.

by SAFRAN (0.7 mm year^{-1} m^{-1}). The gradient was calibrated over approximately one year (from 4 September 2004 to 31 July 2005). There is a good overall coherence between the accumulated precipitation fields forecast by the 24-hour ensemble mean (Figure 4(b)), and that analysed by SAFRAN (Figure 4(a)).

The ESP system has been running daily in real-time mode since 4 September 2004. It produces 51 ten-day streamflow forecasts for about 900 river gauges over France with a three-hour time step. Figure 5(a) shows an example of a graph that can be produced every day for each river station. This shows the ten-day streamflow forecast for the Seine at Paris on the 15 January 2006. The information on the forecast streamflow consists of a plot of the minimum and maximum values within the ensemble (as well as the interval including 80% of the forecast streamflow), the ensemble mean and the control (non-perturbed) run. The observed daily streamflow can be added afterwards.

Figure 5(b) shows a different method of visualising the forecasts, which is similar to the products from EFAS. This chart shows the risk that the forecast streamflow will exceed (or remain below) a given threshold. Each line corresponds to one forecast day, and the lead times are shown in the columns. The percentage of ensemble members for which the forecast streamflow exceeds (or stays below) the threshold is indicated in each of the squares with a specific colour. For example, the chart in Figure 5(b) is for a high flow episode for the Seine river at the Paris gauging station using a threshold of 700 m^3 s^{-1}. This kind of chart allows a quick view of the forecast and provides an alert of a potentially dangerous event. It is of interest, in terms of the follow-up or evaluation of the forecasts, to see if the risk is confirmed from one forecast day to the next.

Figure 5(c) represents an example of the long-term behaviour of the system for the Seine river (at the Paris gauging station) from September 2004 to July 2005. It highlights the overall tendencies of the ensemble forecasts. In this example, the long-term tendency is well reproduced; however the forecast streamflow at the beginning of January 2005 is overestimated.

Statistical analysis of the results of the ensemble streamflow forecast system

The probabilistic nature of ensemble forecasts implies a verification that is quite different from the verification of deterministic forecasts. As it is not possible to evaluate the quality of a single ensemble forecast against a reference, it is necessary to collect long time series of ensemble forecasts and observations, and to use statistical verification methods. We performed the statistical analysis of the ensemble streamflow prediction system over nearly one year, from 4 September 2004 to 31 July 2005.

Precipitation forecasts

First, we focused on the quality of a model input: the downscaled ensemble precipitation forecasts. To do so, we used the SAFRAN analysed precipitation as a reference. This preliminary study indicates that light precipitation events are slightly over-estimated a few days ahead, and the differences clearly become larger over a longer time period. In contrast, high precipitation events are underestimated, with the underestimation growing with the lead time. The spatial (over France) and temporal (over nearly one year) mean of the daily amount of precipitation ranges from 1.96 mm day-1 for the SAFRAN analysis, 2.11 mm day^{-1} for the one-day ensemble mean, and 2.40 mm day^{-1} for the ten-day ensemble mean. The mean square error of the ensemble mean (with the SAFRAN analysis being the reference) varies from 2.71 mm day-1 for one-day ahead to 3.92 mm day-1 for ten-days ahead. It is interesting to note that the mean square error is larger for the control run than for the ensemble mean, with 2.74 mm day^{-1} for the one-day forecasts and 5.04 mm day^{-1} for the ten-day forecasts. No annual cycle could be found in the error, probably because the 2004–2005 year is very dry, with a weaker precipitation annual cycle than for the other years.

The dispersion of the ensemble ranges from 0.53 mm day^{-1} (one-day forecast) to 3.36 mm day^{-1} (ten-day forecast). It seems quite weak for the first two or three forecast days, as these forecasts are really designed for

medium-range forecasts. This fact is confirmed by the Talagrand Histograms (or rank histograms) which are clearly "U" shaped for the first few days of the forecast. This is less clear at the end of the lead time.

The Brier Score is a quite commonly used statistical metric; it is used to measure the performance of ensemble forecasts of dichotomous events (here, the daily precipitation amount exceeding a given threshold). The Brier Scores computed for thresholds ranging from 1 mm day^{-1} to 20 mm day^{-1} are quite good (i.e. near zero), with a slight increase (i.e. deterioration) with increasing lead time.

Finally, no basin appeared to have clearly better statistical scores, although there were generally slightly lower mean square errors for the northern-most basins (Seine, Loire, Brittany, Charente), and slightly larger errors for the mountainous basins in the south (Adour-Garonne, Rhône, South-East basins).

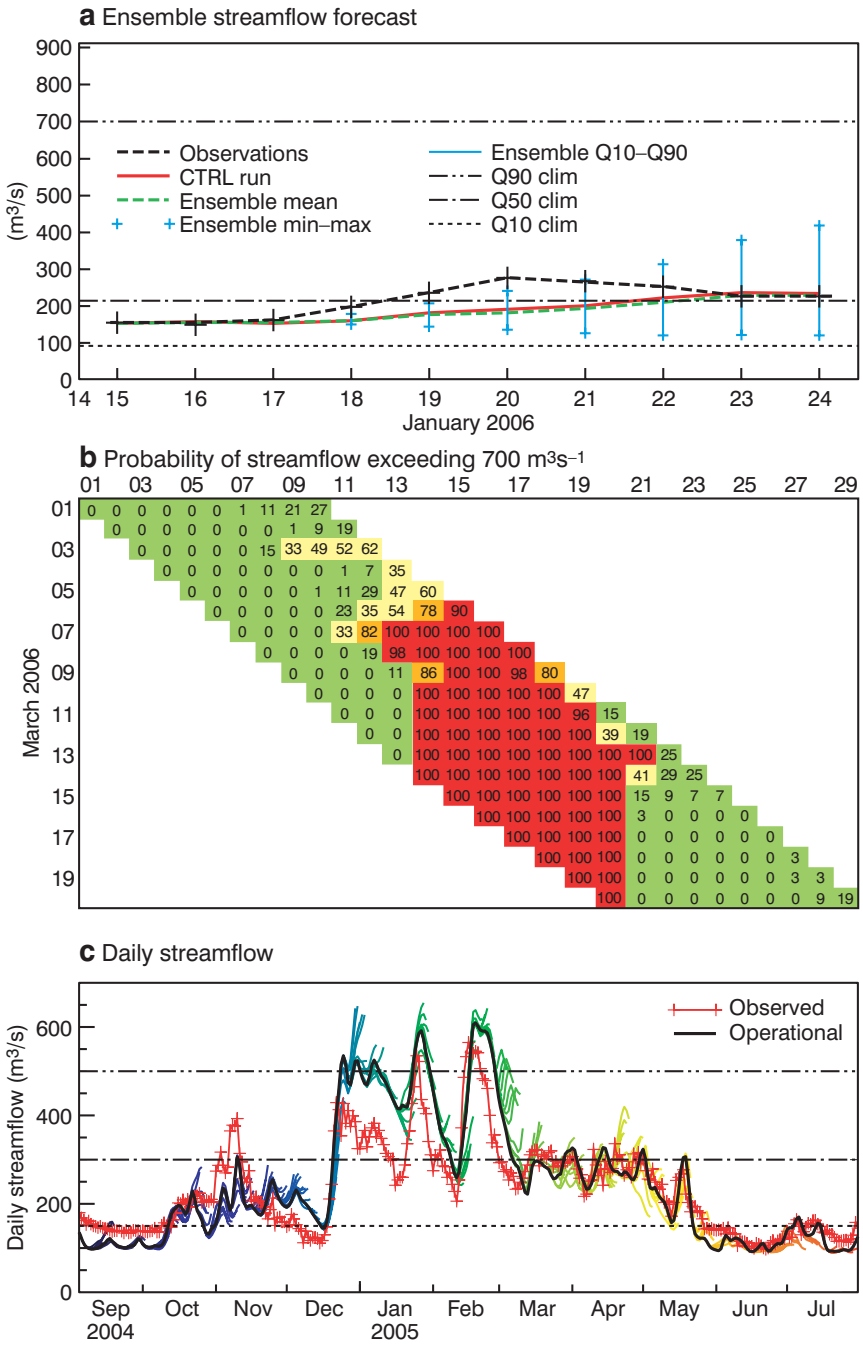

Figure 5 (a) Ensemble streamflow forecast for the Seine at the Paris gauging station, 15 January 2006. (b) Probability of the streamflow exceeding the 700 m^3 s^{-1} level, for the Seine at Paris, forecasts from 1 to 20 March 2006. (c) Daily streamflow of the Seine at the Paris gauging station, from 4 September 2004 to 31 July 2005. Red line with crosses: observed streamflow. Black line: operational streamflow from the operational analysis run of SIM. Other coloured lines: ensemble mean of the ten-day forecast of streamflow starting every day.

Streamflow forecasts

We also performed the statistical analysis for the streamflow forecasts. We focused on high streamflows as well as on low flow periods. As the study period was very dry over France, it provided a good opportunity to test the system for low flows and drought. It should be noted that information concerning low flows is just as important as that for floods for many industries as well as for the various French water management services. In this statistical study the forecast streamflows are compared to a reference run of SIM, and not directly to the observations. This allows the evaluation of only the quality of the ensemble without taking into account neither the hydrological model errors, nor the impact of the anthropogenic effects (especially the dam storage and outflow) that are more significant over a dry year. In the future, it is planned to compare ensemble streamflow forecasts in a more direct manner to the observations, once the improved hydrological-assimilation system based initialisation of SIM is available.

The Talagrand Histograms are generally similar in appearance for all of the river gauges, for example as seen in Figure 6 for the Seine river gauging station at Paris. The "U" shape is clear for the first few days of the forecast, which generally indicates a low ensemble dispersion (see Figure 6(a)). This seems to be mainly linked to the lack of dispersion of the ensemble precipitation for the one-day or two-day ECMWF forecasts. After three or four forecast days, the "U"shape vanishes and the histograms become rather flat, which indicates a good reliability. Sometimes there are particular character- of note: for the

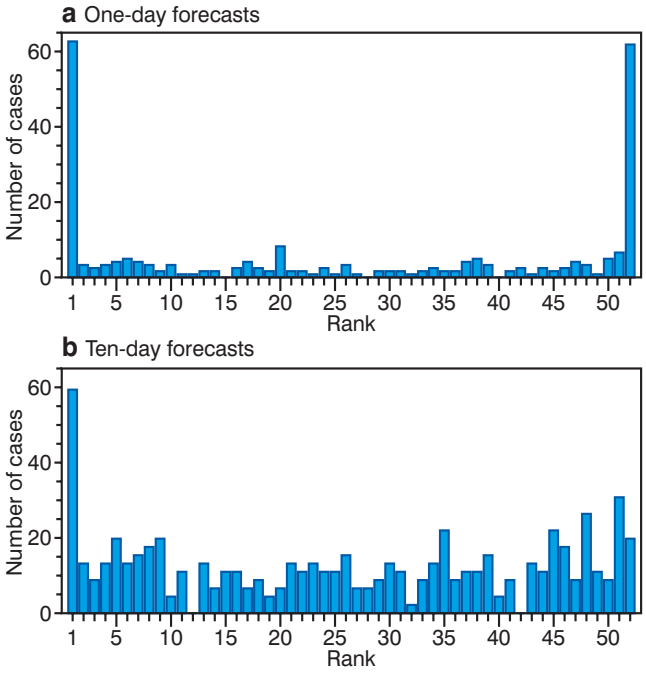

Figure 6 Talagrand Histograms for the Seine at the Paris gauging station, computed from 4 September 2004 to 31 July 2005; with the reference being the operational SIM streamflow: (a) one-day forecasts and (b) ten-day forecasts.

ten-day forecasts, the first rank is predominant which signifies a slight positive bias (see Figure 6(b)).

We computed the Brier Scores for different streamflow thresholds. We focused on high flows by defining the thresholds using the 90th and 50th percentile of daily streamflows from the whole existing climatology, and we also studied low flows by computing the Brier Scores for streamflow remaining below the 10th percentile from climatology. The results are generally good with low values of Brier Scores which slightly increase (i.e. deteriorate) with the lead time.

In order to evaluate the system compared to the climatology (the climatology being computed either with the observed streamflow or with the streamflow analysed by SIM from 1981 to 2004), we computed the Brier Skill Scores. When the Brier Skill Score is close to one, the ESP system provides better forecasts than the climatology. For example, for the Seine river at the Paris gauging station, the Brier Skill Score for the threshold discharge of 300 $m^3 s^{-1}$ ranges from 0.99 (one-day forecast) to 0.8 (ten-day forecast). For all of France (with the climatology being the observed streamflows), the percentage of the 900 river gauges for which the Brier Skill Score is over 0.5 is very close to 100% on the first forecast day for the three thresholds. For ten-day forecasts, the percentages are 82% (>90th percentile), 92% (>50th percentile) and 98% (<10th percentile).

Figure 7 shows the repartition of the Brier Skill Scores as a function of the surface area of the catchments for one-, five- and ten-day forecasts. It reveals that the Brier Skill Scores are closer to unity (i.e. the best possible) for large basins, while the lowest Skill Scores are generally found for the smallest basins. Thus, the Brier Skill Scores tend to decrease (i.e. deteriorate) with increasing lead time. This shows that the system obtains good statistical scores for the majority of the river gauges, both for high as well as for low flow events.

Other statistical measures for evaluating the potential of the ensemble streamflow prediction system are the False Alarm Ratio and the Hit Rate. This kind of information may help ensemble prediction system end-users establish a decision-making system based on the ensemble forecasts, follow their costs and understand the consequences of false alarms or missed forecasts. The idea is to compute a contingency table for streamflow events which exceed a certain threshold. The event is considered as "forecast" when it is forecast by at least 50%, or 70%, or 90% of the ensemble members. Figure 8

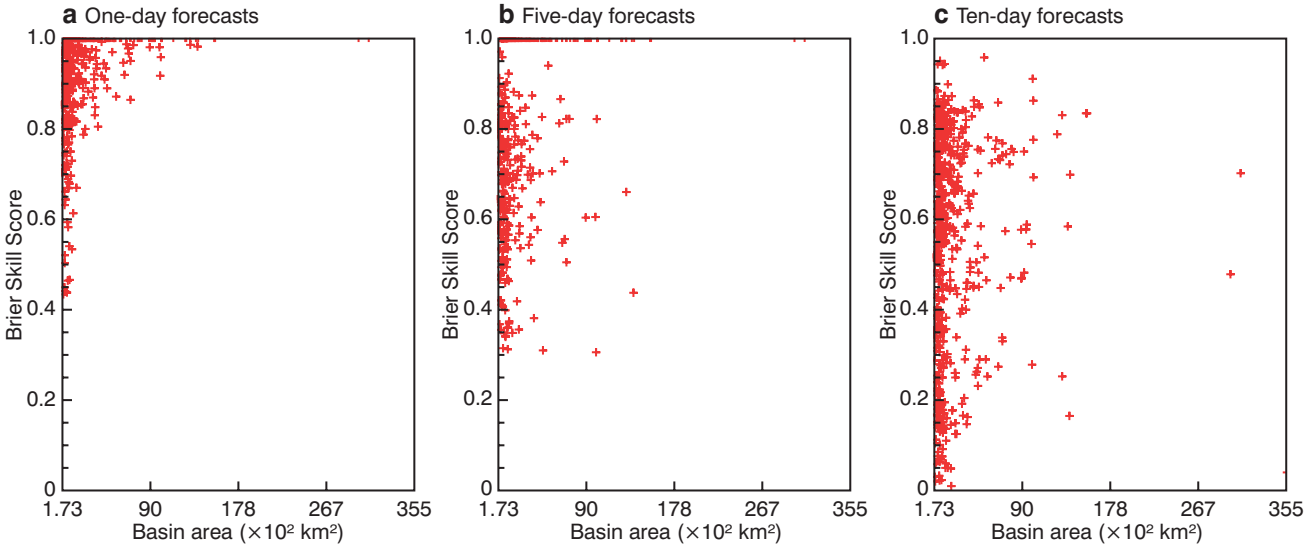

Figure 7 Brier Skill Score, computed from 4 September 2004 to 31 July 2005 using the climatology of 1981–2004 observed riverflows, for a streamflow exceeding the 90th percentile, for 900 river stations over France, following the basin area (km²): (a) one-day forecasts, (b) five-day forecasts and (c) ten-day forecasts.

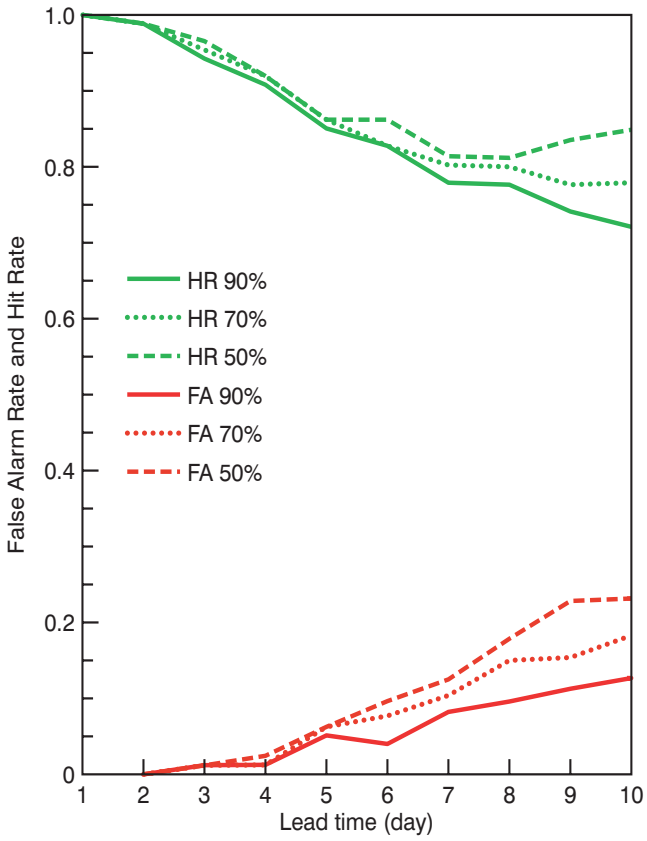

Figure 8 False Alarm Ratio (FA) and Hit Rate (HR) for the Seine at Paris, computed from 4 September 2004 to 31 July 2005 for a streamflow exceeding 300 $m^3 s^{-1}$, following the forecast lead time (from 1 to 10 days).

shows the results for the Seine river at the Paris gauging station for the threshold discharge of 300 $m^3 s^{-1}$. The Hit Rate is quite high (over 0.75) in all of the cases. The False Alarm Rate stays under 0.2 at every lead time, and the ratio of cases which were not forecast stays below 0.35. It is notable that the absence of precipitation is generally well forecast by the ensemble, and consequently the low flows (< 10^{th} percentile) and their duration is also well predicted, with in particular very low False Alarm Rates and good Hit Rates.

Focus on particular flood events

In addition to the statistical study, we focused on a few flood events in the recent past. Here, the results for the March 2001 Seine flood and the September 2006 flood in south-eastern France are presented.

The Seine basin is relatively large (44,000 km^2), with a slow hydrological response and a strong influence of the aquifers (the three main aquifers are explicitly simulated by MODCOU). Figure 9 shows the daily streamflow for the Seine at Paris from 5 March 2001 to 10 April 2001. This long duration flood is well analysed by SIM, as both the observed and the analysed streamflows are very close. The ensemble forecast seems meaningful, generally close to the observed or analysed streamflow, and the dispersion is neither too wide nor too narrow. The increase of the flow is well reproduced by the ensemble. The date of the flood peak also clearly appears in the forecasts, several days ahead, and it is coherent with both the observations and the analysis.

Figure 10 shows the ensemble forecasts for the Herault river at Gignac for the 2006 flood which occurred at the end of September (no observations are available at the current time for this river). This basin is quite small with an area of 1,400 km^2, and there is a very rapid time response to precipitation. Flash floods occur often following strong convective precipitation events. Figure 10(a) shows the forecast issued on 15 September (nine to ten days before the flood), and Figure 10(b) shows the forecast issued on 21 September (three to four days in advance). Figure 10(a) highlights the fact that even if the previous flood is not totally over (i.e. the streamflow is still decreasing), the ensemble forecast is able to give an early warning of the next event. Even if the flood peak is first forecast with an error of one or two days (Figure 10a)) and is underestimated (Figure 10(b)), the information given by the ensemble forecast can be of use for flood warning or water management agencies.

Further developments

The analysis of the downscaled ensemble precipitation forecasts showed good results overall; however there

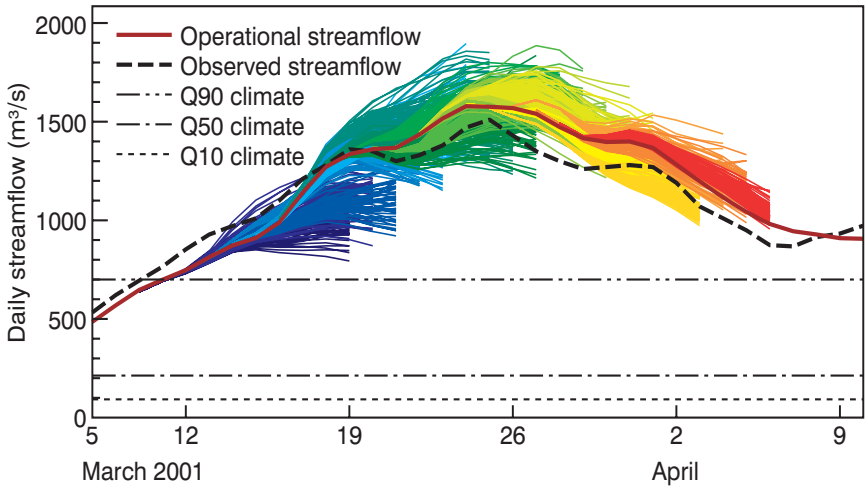

Figure 9 Daily streamflow of the Seine at Paris for the March 2001 ten-year flood. Black dashed line: observed streamflow. Red solid line: streamflow analysed by SIM. Coloured dotted lines: ensemble forecasts from 8 to 27 March 2006. Horizontal black lines: 10^{th}, 50^{th} and 90^{th} percentile of daily streamflow computed from 1974–2006 observed data.

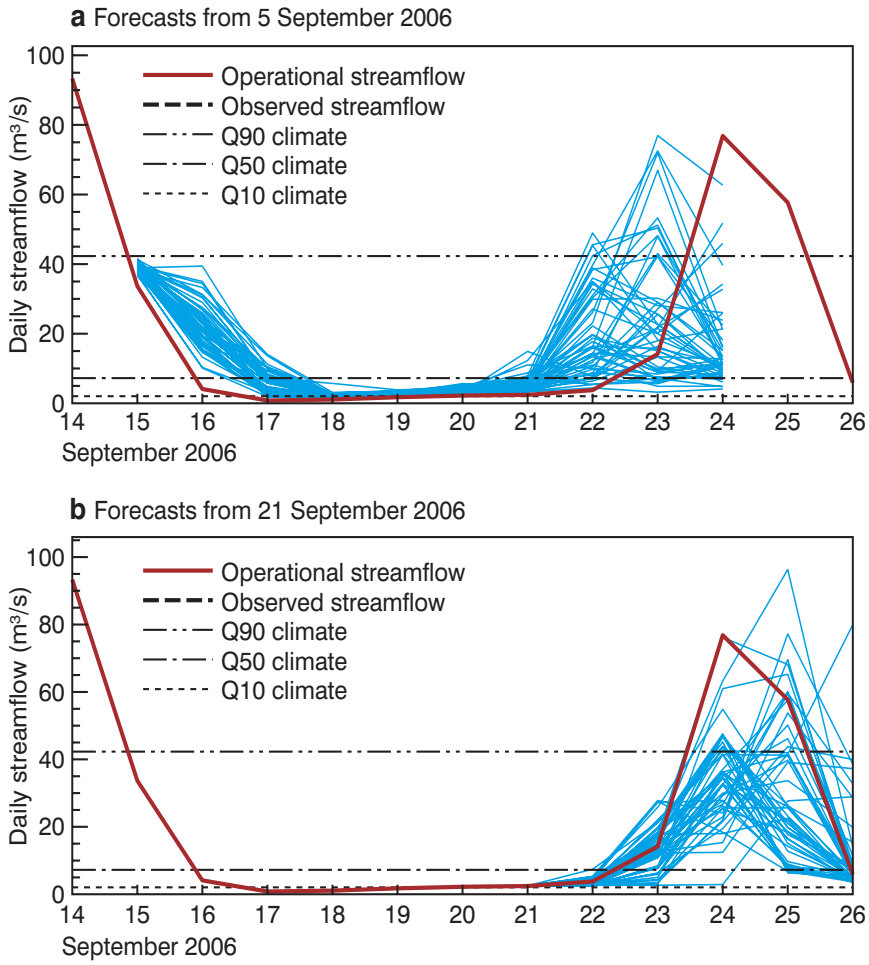

Figure 10 Daily streamflow for the Herault river at Gignac, for the end-September 2006 flood. Red solid line: streamflow analysed by SIM. Blue lines: ensemble forecasts from (a) 15 September 2006 and (b) 21 September 2006. Horizontal black lines: 10th, 50th and 90th percentile of daily streamflow computed from 1989–2006 observed data.

was a slight overestimation of light precipitation and an underestimation of heavy precipitation. Also, there was a lack of dispersion of the ensemble for the first few forecast days. Moreover, the statistical results for the ensemble streamflow forecasts are quite good, with satisfying values for the classical statistical scores (e.g. Brier Score, Ranked Probability Score and Talagrand Histograms). The system gave good results for both high and low flow (the study period being particularly dry) events. In addition consideration of a past flood events revealed that ensemble forecasts can be of great use to hydrological forecasters. This is true in particular for early flood warning for large catchments like the Seine which are characterized by relatively long-duration floods, as well as for smaller basins which have much faster hydrological responses.

In this preliminary study, no ensemble member was associated with perturbations of the physics of SIM or of the hydrological state. The streamflow dispersion was only due to the scatter in the precipitation forcing. Sampling uncertainties related to these hydrological elements is a possible method for improving the ESP system. Moreover, some improvements in the initialisation of SIM are necessary in order to more directly compare the ensemble forecasts and the observations. This is to be accomplished through the development of a hydrological assimilation system. The contribution of the short-range high-resolution meteorological ensemble forecast from Météo-France will also be examined, in particular for the forecasting of the flash floods for relatively small southern French basins.

FURTHER READING

Rousset, F., F. Habets, E. Gomez, P. Le Moigne, S. Morel, J. Noilhan & E. Ledoux, 2004: Hydrometeorological modeling of the Seine basin using the SAFRAN-ISBA-MODCOU system. *J. Geophys. Res.*, **109**, D14105, doi:10.1029/2003JD004403.

Habets F., P. Le Moigne & J. Noilhan, 2004: On the utility of operational precipitation forecasts to served as input for streamflow forecasting. *J. Hydrol.*, **293**, 270–288.

HEPEX web site: http://hydis8.eng.uci.edu/hepex/

EFAS web site: http://efas.jrc.it/

New web products for the ECMWF Seasonal Forecast System-3

FRANCO MOLTENI, LAURA FERRANTI,
MAGDALENA BALMASEDA,
TIM STOCKDALE, FREDERIC VITART

WITH THE implementation of the new seasonal Forecast System 3 in March 2007, the set of graphical products available on the ECMWF web site has been improved and expanded. The purpose of this article is to give a brief overview of the new products available, show some examples of what is available on the web site, and provide some guidance for their use.

A summary of the changes recently introduced is as follows.

a) ***Entry page for the ECMWF forecast products***
www.ecmwf.int/products/forecasts

A new entry has been introduced for the System-3 ocean analysis (*Balmaseda et al.*, 2007), including maps from the real-time and the behind-real-time (BRT) analyses; both are used by the monthly forecast system (*Vitart*, 2003) and the latter by the seasonal forecast system (*Anderson et al.*, 2007). The BRT system is referred to as 'Re-Analysis', since it has been used to assimilate ocean data from January 1959 to the present.

b) ***The seasonal forecast index page***
www.ecmwf.int/products/forecasts/d/charts/seasonal/forecasts

This page leads to three different sections devoted to the 'standard' seasonal-range forecast (run every month up to seven months ahead), the annual-range forecasts (run every 3 months up to 13 months ahead), and the EuroSIP multi-model ensemble made up from integrations of the ECMWF, Météo-France and UK Met Office coupled models.

c) ***The seasonal-range forecast page for System-3***
www.ecmwf.int/products/forecasts/d/charts/seasonal/forecasts/seasonal_range_forecast

This includes entries to the same four categories of products as in System 2, namely plumes for El Niño indices, horizontal maps of three-month anomaly statistics (ensemble mean and probabilities), climagrams (i.e. time series of indices representing area-averaged anomalies or teleconnection pattern amplitudes) and tropical-storm indices. However, all these sections have been improved, and forecast products have been extended to seven months following the increased length of the integrations.

Additions include a new 'summary' plot of probabilities for tercile-based categories in the horizontal map section. There is a substantial expansion of the climagram section, now comprising area-averages of two-metre temperature and precipitation over 25 areas, extratropical teleconnection indices and rainfall-based monsoon indices. Tropical storms indices have been revisited, and a measure of forecast uncertainties has been included.

d) ***The annual-range forecast page for System-3***
www.ecmwf.int/products/forecasts/d/charts/seasonal/forecasts/annual_range_forecast

This page includes entries for three categories of products, namely El Niño plumes, spatial maps and tropical storm statistics. At present the annual-range forecasts are only visible to Member State users.

We will now illustrate some of the new products in greater detail.

The System-3 ocean analysis products

The System 3 (S3) operational ocean analysis consists of two analysis streams: (a) a historical reanalysis from 1 January 1959 which is continuously updated (with a delay of 11 days) and is used to initialize seasonal forecasts, and (b) a real-time ocean analysis, used to initialize the monthly forecasts. The S3 ocean analysis has several innovative features, including an on-line bias correction algorithm, the assimilation of salinity data on temperature surfaces, and assimilation of altimeter-derived sea level anomalies and global trends. The S3 ocean analysis has been running since August 2006, and became fully operational in March 2007.

The new ocean web pages (www.ecmwf.int/products/forecasts/d/charts/ocean) offer, for the first time, products from both the real-time stream and from the historical reanalysis. Online documentation of the ocean analysis system is also available, with information on the observations used, the ocean archive and a guide to the ocean products. The selection of ocean products can be summarized as follows.

- ***Horizontal maps*** of sea surface temperature (SST), sea level (SL), depth of 20°C isotherm (D20), sea surface salinity (SSS), zonal wind stress (Tau-x), and temperature and salinity averaged over the upper 300 m (T300 and S300 respectively). T300 and S300 are proxies for the upper ocean heat and salt content, and D20 is a proxy for the depth of the thermocline.
- ***Zonal sections*** of temperature along the equator.
- ***Meridional sections*** of temperature at 165°E, 140°W and 30°W.
- ***Time-Longitude sections*** along the equator of SST, sea level, depth of 20°C isotherm and zonal wind stress.
- ***Observation coverage maps*** and quality control decisions for subsurface observations. The maps include information about number of profiles, observation type (mooring, ARGO floats, or XBTs), and whether the profile has been fully accepted, rejected, partially rejected or "super-obbed" (a super-observation is the average of several observations correlated in time and space that is given extra weight).

Sections				
Spatial attributes	Parameter	Time attributes		
Horizontal **Global** / Tropical	SST, **SSS**, SL, D20, **T300**, **S300**, Tau-x	Average	Updated / delay	Record
		Daily	**Every day No delay**	Last 30 days
Zonal Equatorial	Temperature	Weekly	Sundays. 11 days delay	From January 2007
Meridional 165°E / 140°W / 30°W	Temperature	**Monthly**	**End of each month. 11 days delay**	**From 1959**
		Span		
Hovmoller Equatorial	SST, SL, D20, Tau-x	Last 6 months	**Every day No delay**	**Latest**
		6 / **12** months	End of each month. 11 days delay	**From 1959**
Observation coverage maps and quality control				
Global maps	**Temperature and salinity profiles**	**10-days assimilation window**	**Every day**	**Last 30 days**
			Every 10 days. 11 days delay	**From 1959**

Table 1 Summary of the ocean analysis products available in the web. Blue indicates products only available from the reanalysis stream, and red products are only available from the real-time stream. Common products are in black. New products are in bold. The abbreviations used for the Parameter are defined in the section on the S3 ocean analysis products.

Both full fields and anomalies are displayed. The anomalies have been calculated respect the 1981–2005 climatology, which is the same period used for the hindcast integrations of the S3 seasonal forecasts. The maps represent daily fields from the real-time analysis, and weekly and monthly fields from the reanalysis stream. The monthly fields go back to 1959 and the weekly fields have only been displayed since January 2007. Table 1 offers a summary of the ocean products on the web. The products only available for the reanalysis are in blue, those that exist only for the real-time stream are in red, and the products common for both streams (although at different timings) are in black. The new products are in bold.

Figure 1 shows longitude-depth sections of temperature along the equator for eight months during the reanalysis period, illustrating the transition from warm to cold conditions in four ENSO events. While normally transitions from warm to cold phases occur on a time scale of one year, the transition during the recent winter (see panels for December 2006 and March 2007) was anomalously rapid.

The 'tercile summary' probability plot

Probabilities of tercile-based categories for three-month mean anomalies have been produced since the introduction of the first operational seasonal forecast system at ECMWF. So far three different maps have been available for individual categories, corresponding to the lower, middle and upper third of the anomaly distribution. To have a proper assessment of the distribution it is necessary to examine at least two of these maps. Alternatively, the user could consult the map for the probability of anomalies being above (or, by difference, below) the median value to get a single-map overview. However, using such a product one must be careful not to confuse high/low probabilities with large positive/negative anomalies!

In most cases, users are interested in spotting regions where significant deviations from climatological values may occur. To provide such information in a synthetic form, a new plot has been introduced with probabilities only plotted in those areas where (a) the highest probability among the three tercile-bounded categories is predicted for one of the two extreme categories and (b) such a probability exceeds 40%. An example of the 'tercile-summary' for the prediction of two-metre temperature in the January–March 2007 period, derived from the pre-operational System-3 forecast started on 1 December 2006, in shown in Figure 2. The prevalence of orange/red colours indicates a moderate to high chance of anomalously warm temperatures over most of the tropics, North Atlantic, Europe and western Asia.

Climagrams: new graphical display for an extended set of indices

As mentioned in the introduction, climagrams are graphical products representing the evolution of the ensemble distribution of monthly-mean anomalies for a specific atmospheric parameter throughout the seasonal forecast range. At the time of writing, four categories of parameters are displayed.

- Area averages of two-metre temperature anomalies.
- Area averages of precipitation anomalies.
- Teleconnection indices based on mean-sea-level pressure or geopotential height anomalies.

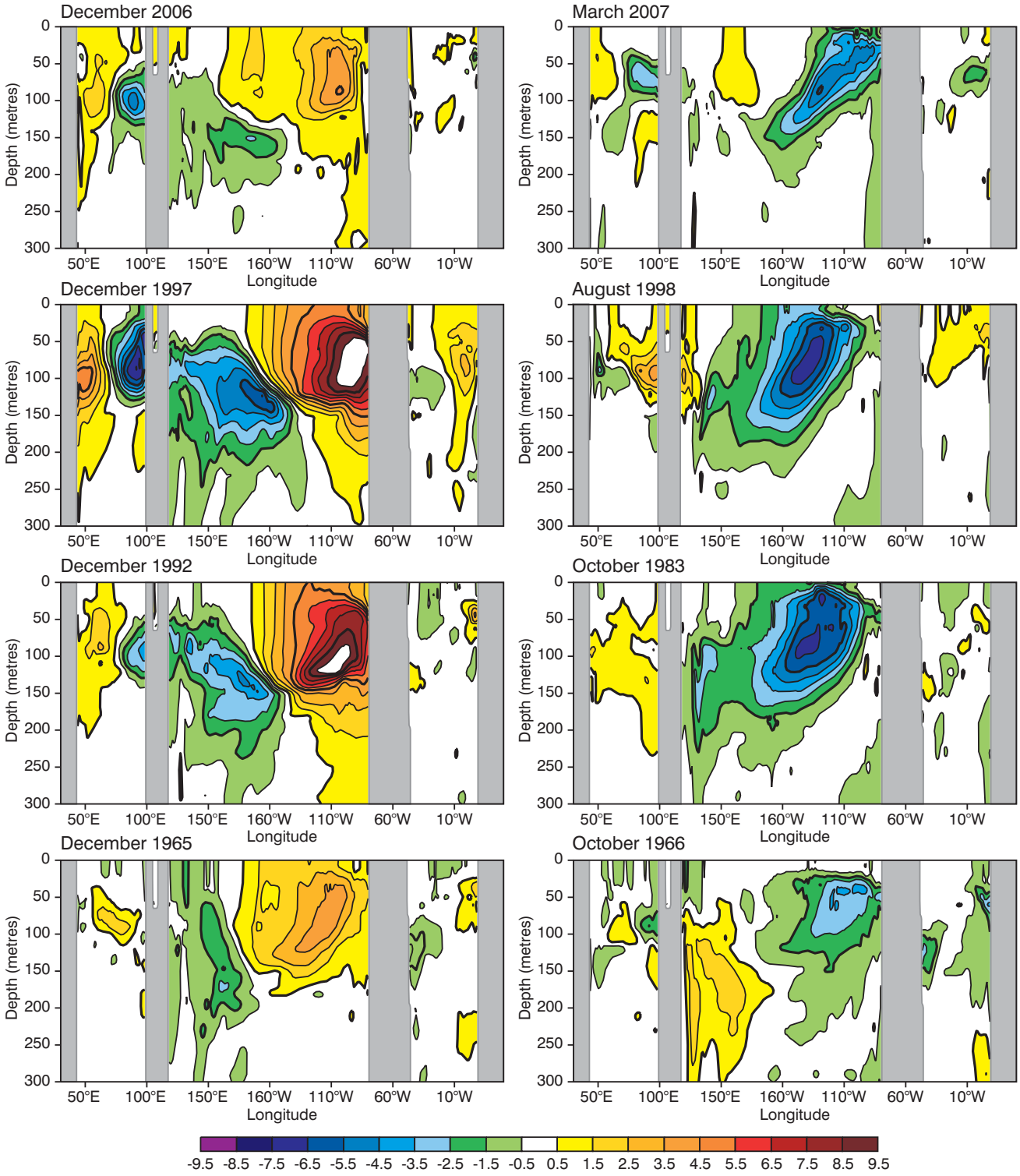

Figure 1 Longitude-depth sections of temperature along the equator for eight months during the S3 ocean reanalysis period, illustrating the transition from warm to cold conditions in four ENSO events. Left column, top to bottom: December 2006, December 1997, December 1982, December 1965. Right column, top to bottom: March 2007, August 1998, October 1983, October 1966.

◆ Monsoon indices based on rainfall anomalies.

Climagrams for SST indices are going to be introduced in the near future.

The new graphical display of the climagrams is illustrated in Figure 3 by two examples. Figure 3(a) shows the predicted distribution of the Equatorial Southern Oscillation Index (ESOI) from a pre-operational forecast started in November 2006, while Figure 3(b) shows the distribution of two-metre temperature anomalies averaged over the Southern European region (35–50°N, 10°W–30°E) from the October 2006 pre-operational forecast.

For each index and each month in the seven-month forecast range, the climagram compares the following three distributions.

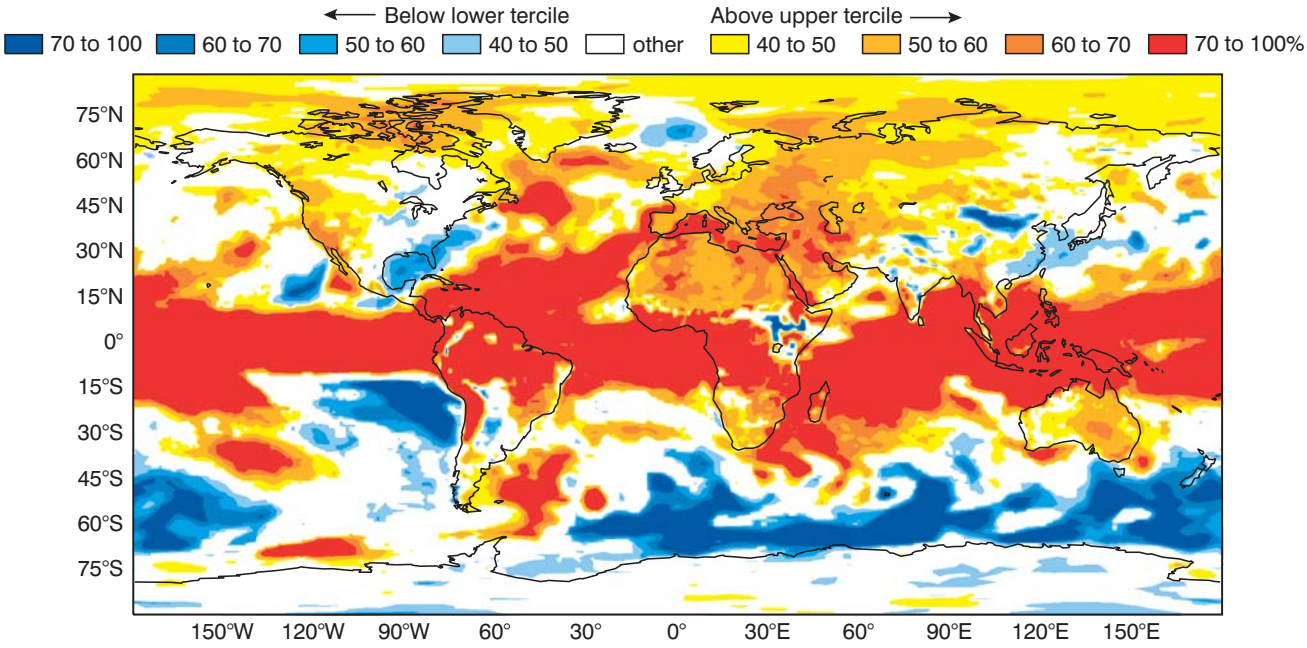

Figure 2 Example of the 'tercile summary' plot for the probabilities of two-metre temperature categories, from the S3 forecast started in December 2006.

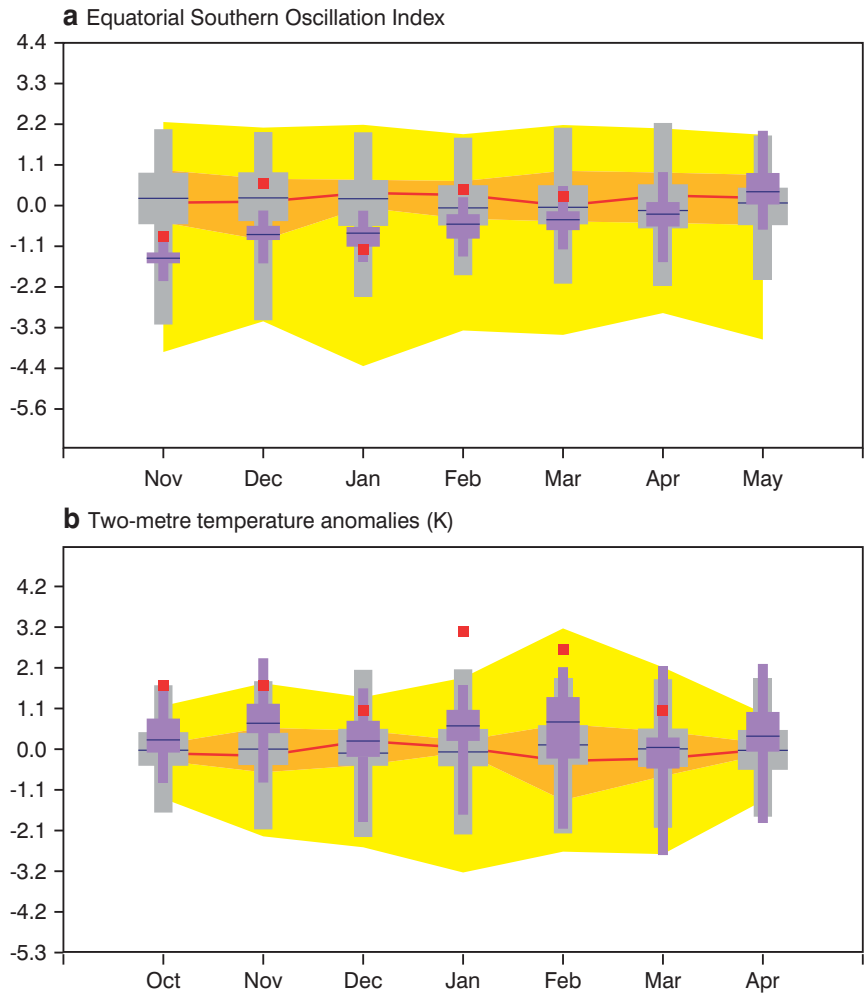

Figure 3 Examples of climagrams for the Equatorial Southern Oscillation Index (top) and the two-metre temperature anomaly averaged over Southern Europe (35°N–50°N, 10°W–30°E; bottom). See the main text for the explanation of the graphical elements.

- The distribution derived from observational datasets (ERA-40, operational analysis or GPCP data) during the S3 hindcast period (1981–2005).
- The distribution corresponding to the model climatology computed from the hindcast dataset.
- The distribution from the 41-member ensemble forecast started at the beginning of the first month in the graph.

For each distribution, the graph shows the median, the interval between the lower and upper terciles, and the interval between the 5th and 95th percentiles. For the observational data, the two intervals are represented respectively by orange and yellow bands, with a solid line indicating the median. For forecast data, the two intervals are shown by a box and whiskers of different colour and width: grey and wider for the model climatology, purple and thinner for the actual seasonal forecast. Again, a solid line within the tercile box indicates the median of the distribution. Verification data available *a posteriori* are shown by a red square.

Contrary to the spatial maps for probabilities illustrated in the previous section, climagrams do not classify forecast anomalies in pre-defined

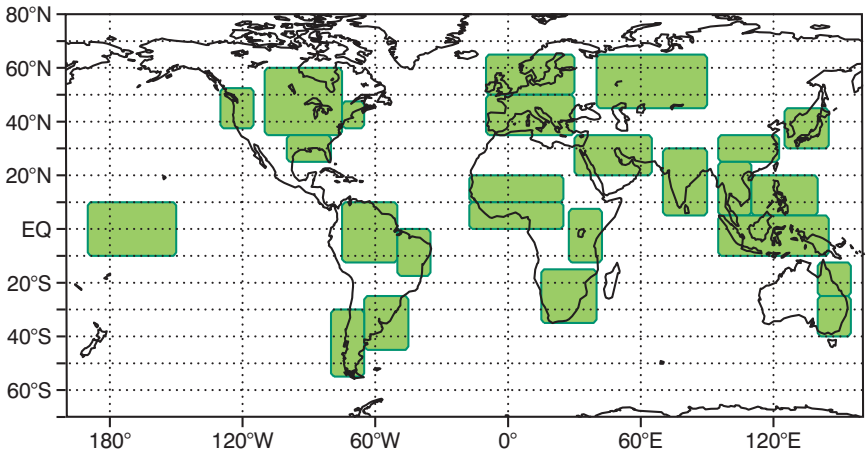

Figure 4 Distributions of areas covered by the climagrams for two-metre temperature and precipitation anomalies.

categories, but rather compare the forecast and climatological distributions in graphical form. This gives the user a visual impression of the difference between the forecast distribution and its climatology, and therefore of the significance of the predicted anomalies. Also, by comparing the model climatological distribution with the observed one, a user gets information about the ability of the forecast model to reproduce the observed anomaly range.

One may wonder whether there is any predictive information in the monthly values displayed in the climagrams, or whether one should only consider three-month means as in the categorical probability maps. If one thinks in terms of, say, correlations of anomalies for a specific month across the 25-year hindcast range, in the large majority of cases such a correlation turns out to be lower than the correlation for three-month means centred on that specific month. However, if one considers the relative variations of monthly anomalies within the seven-month period, it is found that, in a number of cases, such variations had a counterpart in the observations. For example, the recent transition from a warm to a cold ENSO phase in the eastern tropical Pacific (corresponding to the decrease and eventual reversal of ESOI anomalies in Figure 3(a)) caused significant intra-seasonal variations in the northern hemisphere circulation, which were often captured by the seasonal forecast. In Figure 3(b), not only the overall positive sign of the temperature anomaly over Southern Europe in the last autumn/winter was predicted by the October forecast, but also some of the intraseasonal fluctuations (although with a lower degree of consistency between successive forecasts).

Finally, we wish to point out that the number of areas for which two-metre temperature and rainfall anomalies are displayed in the climagrams has been substantially increased with respect to the previous seasonal forecast system, with a more extensive coverage of tropical and southern mid-latitude regions. The full set of areas is illustrated in Figure 4.

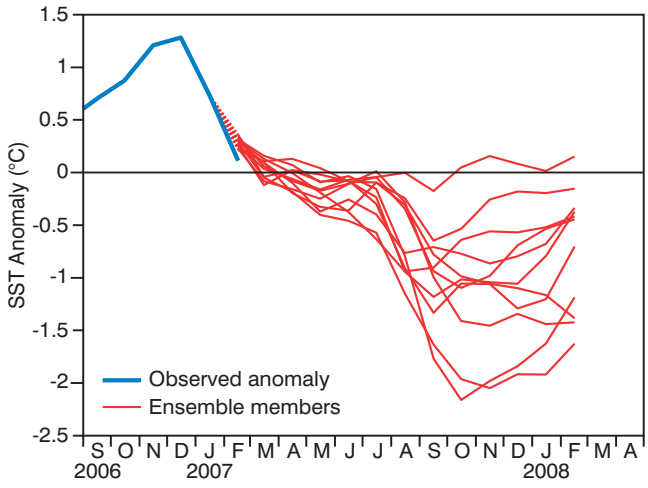

Figure 5 Niño 3.4 (120°W–170°W, 5°N–5°S) SST anomaly from the annual-range forecast starting on the 1 February 2007. Red lines are the individual forecast ensemble members and the blue line is the observed anomaly to date.

The annual range forecasts

An example of a Nino 3.4 SST forecast plume from the latest annual range forecast is given in Figure 5. The reduced ensemble size of the annual range forecasts (11 members) limits the usefulness of forecasts of noisy fields such as precipitation, but is sufficient to look at the evolution of El Niño. Here the forecast shows that a "La Niña" event (East Pacific SSTs colder than normal) is likely in the second half of this year, but that its amplitude is uncertain at this stage.

What next?

ECMWF has been issuing global seasonal predictions every month since 1997. In 2000 the seasonal forecasts became part of the operational products, and by mid-2000 some of those products became available to all WMO Members. Recently ECMWF has been recognized by the WMO as one of the Global Producing Centres for Long-Range Forecasts (GPCs). Consistent with the role of a GPC, we hope that the new products available from the ECMWF website may be of benefit not only to the ECMWF Member States, but also to international organizations involved in providing guidance on climate-sensitive applications for developing countries.

The set of products described in this article may be further expanded in the future according to users' needs. Also, a set of verification statistics will soon be made available on the web site. We wish to point out that some of these new products (particularly those from the annual-range forecast) should be considered as experimental, and may be modified according to operational experience. In order to progress with the product development, we believe that feedbacks from both operational and research communities are essential, and we encourage all seasonal forecast users to share with us their experience regarding the products described in this article.

FURTHER READING

Anderson, **D.**, **T. Stockdale**, **M. Balmaseda**, **L. Ferranti**, **F. Vitart**, **F. Molteni**, **F. Doblas-Reyes**, **K. Mogensen** & **A. Vidard**, 2007: Development of the ECMWF Seasonal Forecast System-3. *ECMWF Tech. Memo. No. 503.*

Balmaseda, **M.**, **A. Vidard** & **D. Anderson**, 2007: The ECMWF System-3 ocean analysis system. *ECMWF Tech. Memo. No. 508.*

Vitart, **F.**, 2003: Monthly forecasting system. *ECMWF Tech. Memo. No. 424.*

ECMWF Calendar 2007

June 4–8	Training Course – Use and interpretation of ECMWF products
June 11–13	Workshop – Flow-dependent aspects of data assimilation
June 13–15	Forecast Products – Users' Meeting
June 28–29	Council (*67th Session*)
August 28–31	Eumetcal Workshop
September 3–7	Seminar – Recent developments in the use of satellite observations in numerical weather prediction
October 8–10	Scientific Advisory Committee (*36th Session*)
October 10–12	Technical Advisory Committee (*37th Session*)
October 15–19	Training Course – Use and interpretation of ECMWF products for WMO Members
October 15–16	Finance Committee (*79th Session*)
October 17–18	Policy Advisory Committee (*26th Session*)
October 26	Advisory Committee of Co-operating States (*13th Session*)
November 7–9	Workshop – Ensemble prediction
November 12–16	Workshop – Meteorological Operational Systems (*11th Workshop*)
December 10–11	Council (*68th Session*)

ECMWF publications (see http://www.ecmwf.int/publications/)

Technical Memoranda

524 **Abdalla**, **S.**: Ku-band radar altimeter surface wind speed algorithm. *April 2007*

521 **Weisheimer**, **A.**, **F. Doblas-Reyes**, **P. Rogel**, **E. Da Costa**, **N. Keenlyside**, **M. Balmaseda**, **J. Murphy**, **D. Smith**, **M. Collins**, **B. Bhaskaran** & **T. Palmer**: Initialisation strategies for decadal hindcasts for the 1960–2005 period within the ENSEMBLES project. *March 2007*

520 **Tremolet**, **Y.**: Model error estimation in 4D-Var. *March 2007*

518 **Rodwell**, **M.J.** & **T.N. Palmer**: Using NWP to assess climate models. *March 2007*

516 **Buizza**, **R.**, **H. Asensio**, **G. Balint**, **J. Bartholmes**, **J. Bliefernicht**, **K. Bogner**, **F. Chavaux**, **A. de Roo**, **J. Donnadille**, **V. Ducrocq**, **C. Edlund**, **V. Kotroni**, **P. Krahe**, **M. Kunz**, **K. Lacire**, **M. Lelay**, **C. Marsigli**, **M. Milelli**, **A. Montani**, **F. Pappenberger**, **D. Rabufetti**, **M.-H. Ramos**, **B. Ritter**, **J.W. Schipper**, **P. Steiner**, **J. Thielen-Del Pozzo** & **B. Vincendon**: EURORISK/PREVIEW report on the technical quality, functional quality and forecast value of meteorological and hydrological forecasts. *February 2007*

515 **Benedetti**, **A.** & **M. Janisková**: Assimilation of MODIS cloud optical depths in the ECMWF model. *April 2007*

514 **Leutbecher**, **M.** & **T.N. Palmer**: Ensemble forecasting. *February 2007*

513 **Cardinali**, **C.**, **R. Buizza**, **G. Kelly**, **M. Shapiro** & **J.-N. Thépaut**: The value of targeted observations - Part III: Influence of different weather regimes. *February 2007*

512 **Buizza**, **R.**, **C. Cardinali**, **G. Kelly** & **J.-N. Thépaut**: The value of targeted observations - Part II: The value of observations taken in singular vectors-based target areas. *February 2007*

511 **Kelly**, **G.**, **J.-N. Thépaut**, **R. Buizza** & **C. Cardinali**: The value of targeted observations – Part I: Data denial experiments for the Atlantic and the Pacific. *February 2007*

509 **Bidlot**, **J.-R.**, **P. Janssen** & **S. Abdalla**: A revised formulation of ocean wave dissipation and its model impact. *January 2007*

508 **Balmaseda**, **M.**, **A. Vidard** & **D. Anderson**: The ECMWF System 3 ocean analysis system. *February 2007*

503 **Anderson, D., T. Stockdale, M. Balmaseda, L. Ferranti, F. Vitart, F. Molteni, F. Doblas-Reyes, K. Mogenson & A. Vidard**: Development of the ECMWF seasonal forecast System 3. *April 2007*

ECMWF-ARM Report Series

3 **Neggers, R.A.J.**: A dual mass flux framework for boundary layer convection. Part II: Clouds. *March 2007*

2 **Neggers, R.A.J., M. Köhler & A. Beljaars**: A dual mass flux framework for boundary layer convection. Part I: Transport. *March 2007*

Index of past newsletter articles

This is a selection of articles published in the ECMWF Newsletter series during the last five years. Articles are arranged in date order within each subject category. Articles can be accessed on the ECMWF public web site – www.ecmwf.int/publications/newsletter/index.html

Useful names and telephone numbers within ECMWF

Telephone
Telephone number of an individual at the Centre is:
International: +44 118 949 9 + three digit extension
UK: (0118) 949 9 + three digit extension
Internal: 2 + three digit extension
e.g. the Director's number is:
+44 118 949 9001 (international),
(0118) 949 9001 (UK) and 2001 (internal).

E-mail
The e-mail address of an individual at the Centre is:
firstinitial.lastname@ecmwf.int
e.g. the Director's address is: D.Marbouty@ecmwf.int
For double-barrelled names use a hyphen
e.g. J-N.Name-Name@ecmwf.int

Internet web site
ECMWF's public web site is: http://www.ecmwf.int

	Ext
Director	
Dominique Marbouty	001
Deputy Director & Head of Research Department	
Philippe Bougeault	005
Head of Operations Department	
Walter Zwieflhofer	003
Head of Administration Department	
Ute Dahremöller	007
Switchboard	
ECMWF switchboard	000
Advisory	
Internet mail addressed to Advisory@ecmwf.int	
Telefax (+44 118 986 9450, marked User Support)	
Computer Division	
Division Head	
Isabella Weger	050
Computer Operations Section Head	
Sylvia Baylis	301
Networking and Computer Security Section Head	
Rémy Giraud	356
Servers and Desktops Section Head	
Richard Fisker	355
Systems Software Section Head	
Neil Storer	353
User Support Section Head	
Umberto Modigliani	382
User Support Staff	
Paul Dando	381
Anne Fouilloux	380
Dominique Lucas	386
Carsten Maaß	389
Pam Prior	384
Computer Operations	
Call Desk	303
Call Desk email: calldesk@ecmwf.int	
Console – Shift Leaders	803
Console fax number +44 118 949 9840	
Console email: newops@ecmwf.int	
Fault reporting – Call Desk	303
Registration – Call Desk	303
Service queries – Call Desk	303
Tape Requests – Tape Librarian	315

	Ext
Meteorological Division	
Division Head	
Horst Böttger	060
Meteorological Applications Section Head	
Alfred Hofstadler	400
Data and Services Section Head	
Baudouin Raoult	404
Graphics Section Head	
Jens Daabeck	375
Meteorological Operations Section Head	
David Richardson	420
Meteorological Analysts	
Antonio Garcia-Mendez	424
Anna Ghelli	425
Claude Gibert (web products)	111
Fernando Prates	421
Meteorological Operations Room	426
Data Division	
Division Head	
Adrian Simmons	700
Data Assimilation Section Head	
Erik Andersson	627
Satellite Data Section Head	
Jean-Nöel Thépaut	621
Re-Analysis Project (ERA) Head	
Saki Uppala	366
Probabilistic Forecasting & Diagnostics Division	
Division Head	
Tim Palmer	600
Seasonal Forecasting Section Head	
Franco Molteni	108
Model Division	
Division Head	
Martin Miller	070
Numerical Aspects Section Head	
Agathe Untch	704
Physical Aspects Section Head	
Anton Beljaars	035
Ocean Waves Section Head	
Peter Janssen	116
GMES Coordinator	
Anthony Hollingsworth	824
Education & Training	
Renate Hagedorn	257
ECMWF library & documentation distribution	
Els Kooij-Connally	751